JAHRBUCH DER GEOLOGISCHEN BUNDESANSTALT
Jb. Geol. B.-A. | ISSN 0016-7800 | Band 140 | Heft 4 | S. 9–28 | Wien, September 1997

Geophysical Investigations in the Southern Bohemian Massif

KAY ARIC, RUDOLF GUTDEUTSCH, HERBERT HEINZ†, BRUNO MEURERS, WOLFGANG SEIBERL, ANTAL ÁDÁM & DAVID SMYTHE*)

17 Text-Figures, 4 Tables and 2 Plates (in pocket)

Tschechische Republik
Niederösterreich
Böhmische Masse
Geophysik
Seismik
Schweremessung
Magnetotellurik
Magnetik
Radiometrie

Österreichische Karte 1 : 50.000
Blätter 1–9, 12–22, 29–38, 51–54

Inhalt

Geophysikalische Untersuchungen in der südlichen Böhmischen Masse

Zusammenfassung

Tiefenseismische Untersuchungen und die Auswertung teleseismischer Ereignisse in ausgesuchten Gebieten deuten auf eine eher reflexionsarme Oberkruste hin. Starke Reflexionen wurden in der Unterkruste und im Bereich der Moho (34 km) beobachtet. Für den Übergang vom Moravikum zum Moldanubikum im Bereich des Messerner Bogens wird ein komplexes Modell vorgestellt, das seismische und magnetotellurische Daten zusammen mit geologischen Informationen interpretiert. Das Moldanubikum ist konkordant auf das Moravikum überschoben. Der Bittesche Gneis, die phyllitischen Glimmerschiefer bzw. die Paragneise unterlagern die Bunte Serie und zeigen eine abtauchende Tendenz. Die Hauptquellen gravimetrischer und magnetischer Anomalien sind der oberen Kruste zuzuordnen. Das regionale Anomalienmuster korreliert mit den wichtigsten tektonischen Einheiten. Der Dichtekontrast zwischen Südböhmischem Pluton und den benachbarten metamorphen Gesteinen prägt die regionale Verteilung der Bouguer-Schwere. Die charakteristische Bouguer-Anomalie zwischen Retz und Hollabrunn ist auf die Überlagerung der Schwerewirkung des Thaya-Plutons und der Molasse-Sedimente zurückzuführen. Zweidimensionale Modelle werden vorgestellt. Die aeromagnetische Karte zeigt innerhalb der Granit-Intrusion einen sehr ruhigen Verlauf, während die metamorphen Einheiten des Moldanubikums und Moravikums durch eine dichte Folge lokaler Anomalien mit teilweise großer Amplitude gekennzeichnet sind. Die magnetische Anomalie bei Liebenau wird von steil einfallenden Kontaktzonen zwischen verschiedenen Granittypen verursacht. Diese Zonen zeigen außerdem Kalium- und teilweise auch Thoriumanreicherungen.

*) Authors' addresses: Dr. KAY ARIC, Dr. RUDOLF GUTDEUTSCH, BRUNO MEURERS, Dr. WOLFGANG SEIBERL, Institute of Meteorology and Geophysics, University of Vienna, Hohe Warte 38, A-1190 Vienna and Althanstraße 14, A-1090 Vienna, Austria; Dr. HERBERT HEINZ†, Geologische Bundesanstalt, Rasumofskygasse 23, POB 127, A-1031 Vienna, Austria; ANTAL ÁDÁM, Geodetical and Geophysical Research Institute of the Hungarian Academy of Sciences, Csatka E. u. 6–8, H-9400 Sopron, Hungary; DAVID SMYTHE, Department of Geology & Applied Geology, University of Glasgow, Glasgow G12 8QQ, Scotland.

Abstract

Seismic soundings and the observation of teleseismic events in selected areas indicate a rather homogeneous crust within large complexes of the Southern Bohemian Massif. The Mohorovicic-discontinuity appears as a strong reflector in a depth of 34 km. Regarding local aspects the most important results are as follows. In the Messern Arc Moldanubian (Dobra gneiss) and Moravian (Bittescher gneiss) are separated through the rocks of the Variegated Sequences (Bunte Serie). Two different tectonic hypotheses are favoured. A concordant overthrusting of Moravian formations is a possible interpretation. This model fits best the geological and geophysical data. The main sources both of the magnetic and gravity anomalies are due to upper crustal structures. Within wide areas the regional anomaly pattern coincides well with tectonic structures observed by surface geology. The gravity reflects the lower density of the granitic intrusions in contrast to high density metamorphic rocks. Several two-dimensional models are presented. The negative-positive gravity anomaly couple in the area between Retz and Hollabrunn is explained by combined gravity effects of the Thaya pluton and the Molasse basement. The aeromagnetic map shows quiet signatures within the granite intrusion while a dense sequence of partly high amplitude anomalies is observed within the metamorphic part of Moldanubian and Moravian units. The sources of magnetic anomalies near Liebenau are steeply dipping contact zones between different granite types. These zones are also indicated by enrichments in potassium and partly in thorium.

1. Introduction

The main target of the geophysical investigations in the Southern Bohemian Massif (SBM) was to clarify certain structural and tectonic settings. Following geophysical methods were applied (see Text-Fig. 1):

- reflection and refraction seismics near St. Martin (SW of Gmünd) and Messern (Horn)
- magnetotellurics and audiomagnetotellurics near Messern
- seismological observations near Zwettl
- gravimetry
- magnetics
- radiometrics.

The corresponding data were compiled from already existing data as well as from data collected during the current investigations. The new gravity station net is shown in Text-Fig. 1. The complete area has been covered in the past by a regional aeromagnetic survey. A detailed investigation using magnetic and radiometric data from a helicopter survey was carried out near Liebenau (Text-Fig. 1).

2. Seismic Investigations

This section deals with the localisation of the boundary between the Moldanubian and Moravian units next to the Messerner Bogen (see Text-Figs. 1 and 2). From the geological point of view it is interesting which relation exists between Bittescher gneiss in the East, being part of the Moravian, and the Dobragneiss underlying the Granulite in the West. WIESENEDER & FREILINGER (1976) describe remarkable similarities of both units. MATURA (FUCHS & MATURA, 1976, 1980) suggests a linking trough-shaped structure, which excludes the model of a thrust fault between Moldanubian and Moravian in the area West of Messern. Contrary FUCHS (1976) and THIELE (1976) assume overthrusting of Bittescher gneiss which implies that no genetic relation exists between both rock sequences. This question has been subject to combined seismic and magnetotelluric investigations. Text-Fig. 2 (Geol. B.-A., 1984) shows the locations of the refraction and reflection seismic measurements performed to resolve shallow structures down to 2000 m depth.

2.1. Shallow Refraction and Reflection Seismics in the Area of the Messerner Bogen

A 24-channel digital acquisition system with 72 dB dynamic range has been used. A special device of vacuum-assisted weight drop was applied as seismic source (BRÜCKL, 1988) in the following shot – geophone pattern:

- 40 m spacing of geophone groups
- 10 m seismic source interval
- 16-fold vertical stacking of the weight drop.

Each geophone group consisted of twelve 30 Hz geophones with an array length of 20 m. The geophone gather

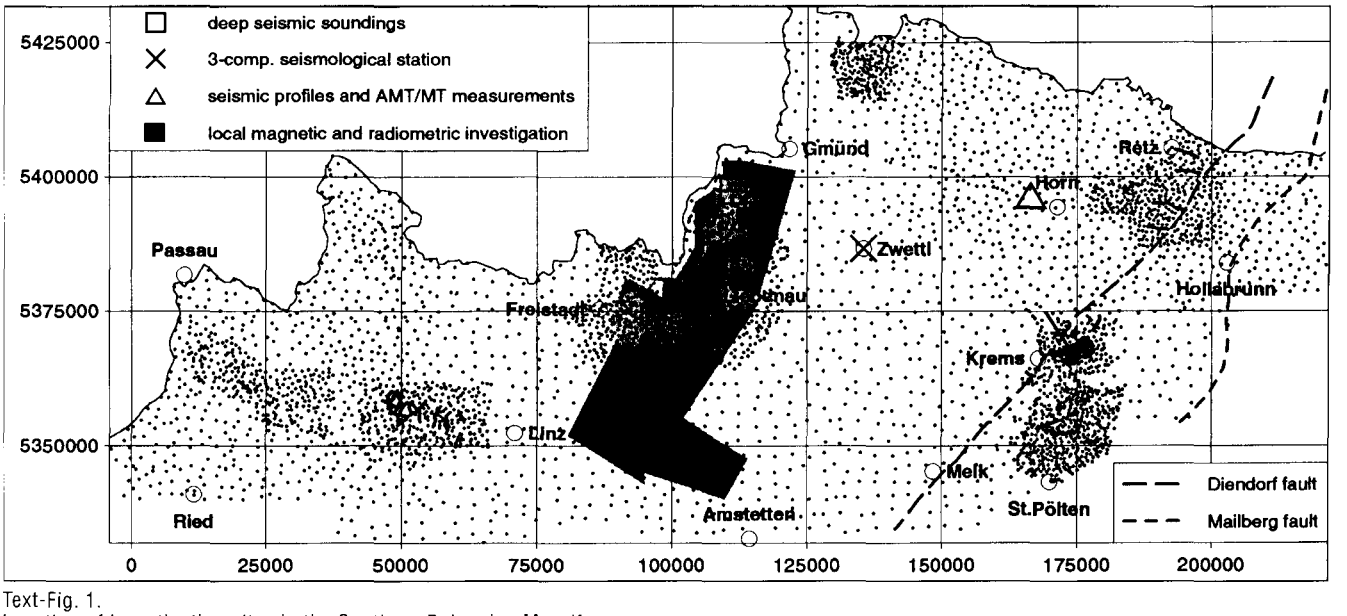

Text-Fig. 1.
Location of investigation sites in the Southern Bohemian Massif.
Explanation see text.

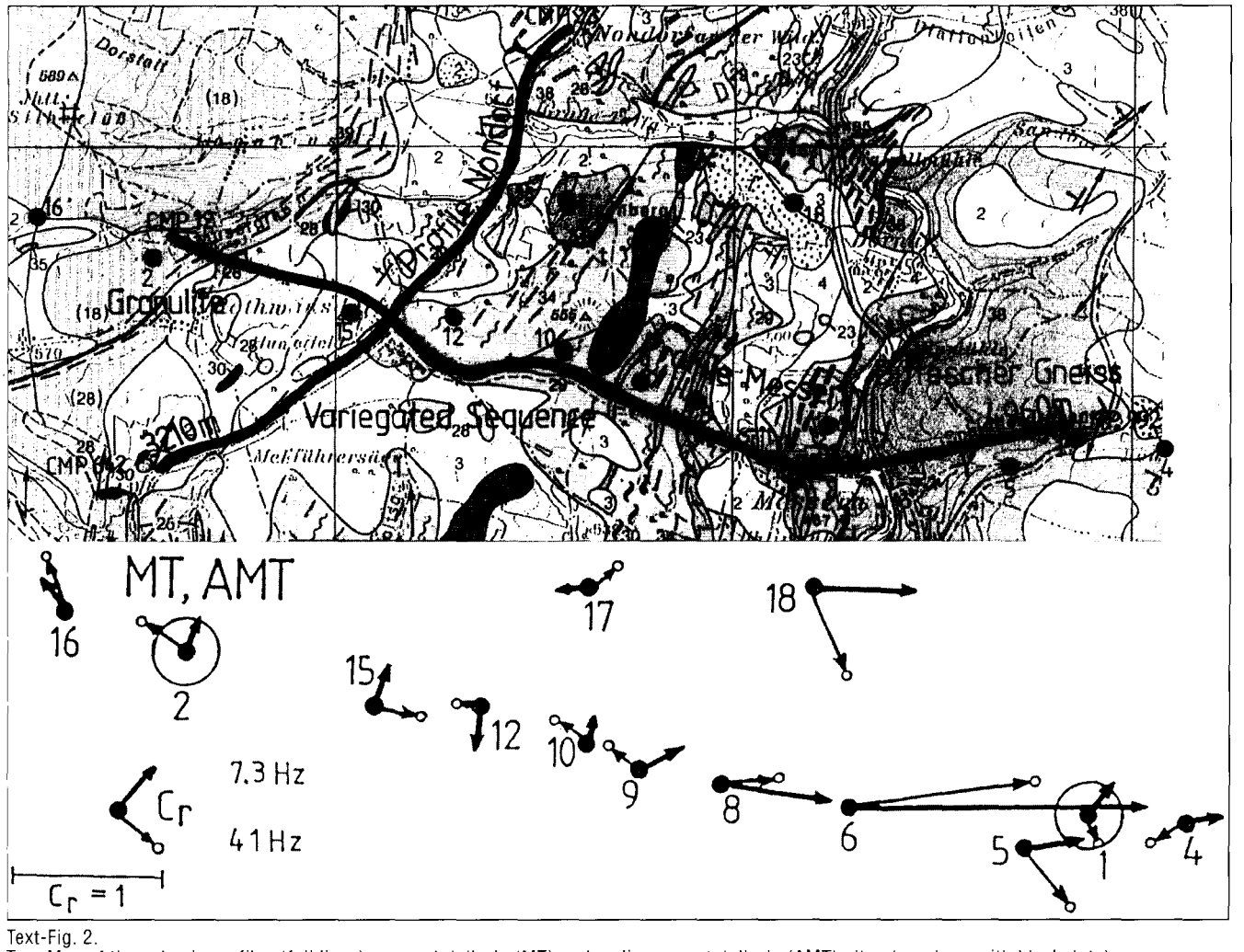

Text-Fig. 2.
Top: Map of the seismic profiles (full lines), magnetotelluric (MT) and audio-magnetotelluric (AMT) sites (numbers with black dots). Geology after FUCHS & MATURA (1984).
The numbers at each end of the seismic profiles indicate CMPs points (interval = 5 m). Indications of geological units: 1–4 = Quaternary sediments; 18 = granulite; 23 = marble; 27 = quarzite; 28 = paragneiss; 29 = mica schists; 30 = paragneiss with graphite; 34 = paragneiss with amphibolite; 37 = granitic gneiss; 38 = Bittescher gneiss; 39 paragneiss.

Bottom: Real components (Cr) of the induction vectors at two frequencies 7.3 and 41 Hz.

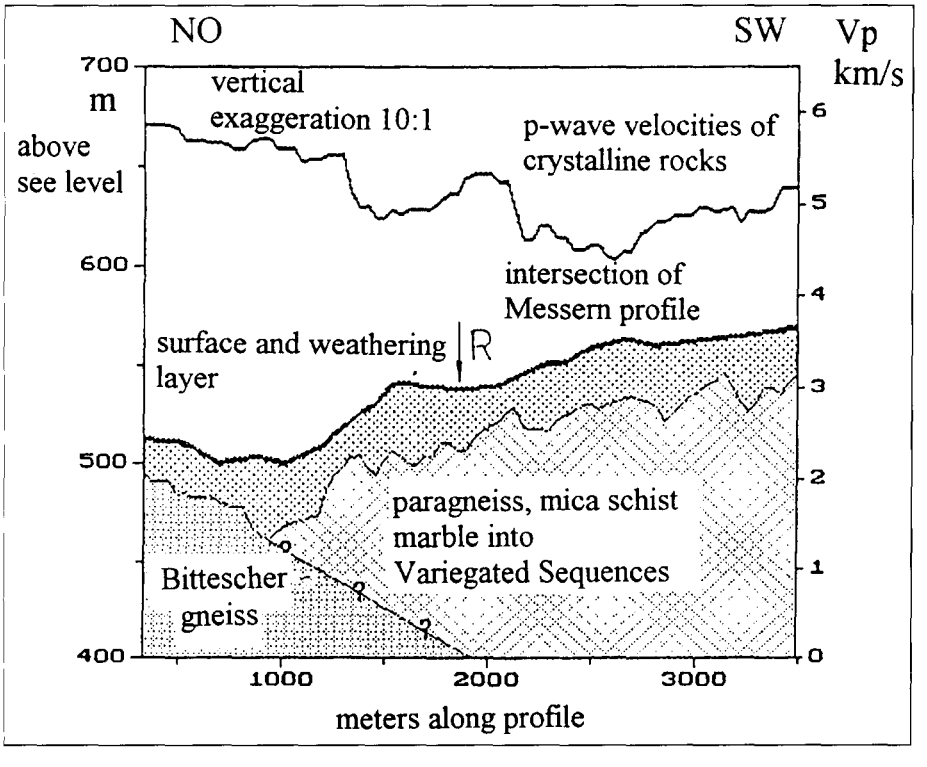

Text-Fig. 3.
Messern refraction seismic profile.
Topography, thickness of Quaternary sediments, P-wave velocity of the crystalline rocks.
R: intersection of Nondorf profile.

includes 96 traces with a spacing of 10 m between each field record (CGP-sorting). The co-ordinates of the geophone sites were controlled by geodetic surveying.

The P-wave velocity in the Quaternary cover ($V_p = 0.6 \pm 0.1$ km/s) and the crystalline rocks were obtained from the first arrival travel times. The GRM-method developed by PALMER (1981) has been applied. Due to the length of the seismic profiles and the relatively

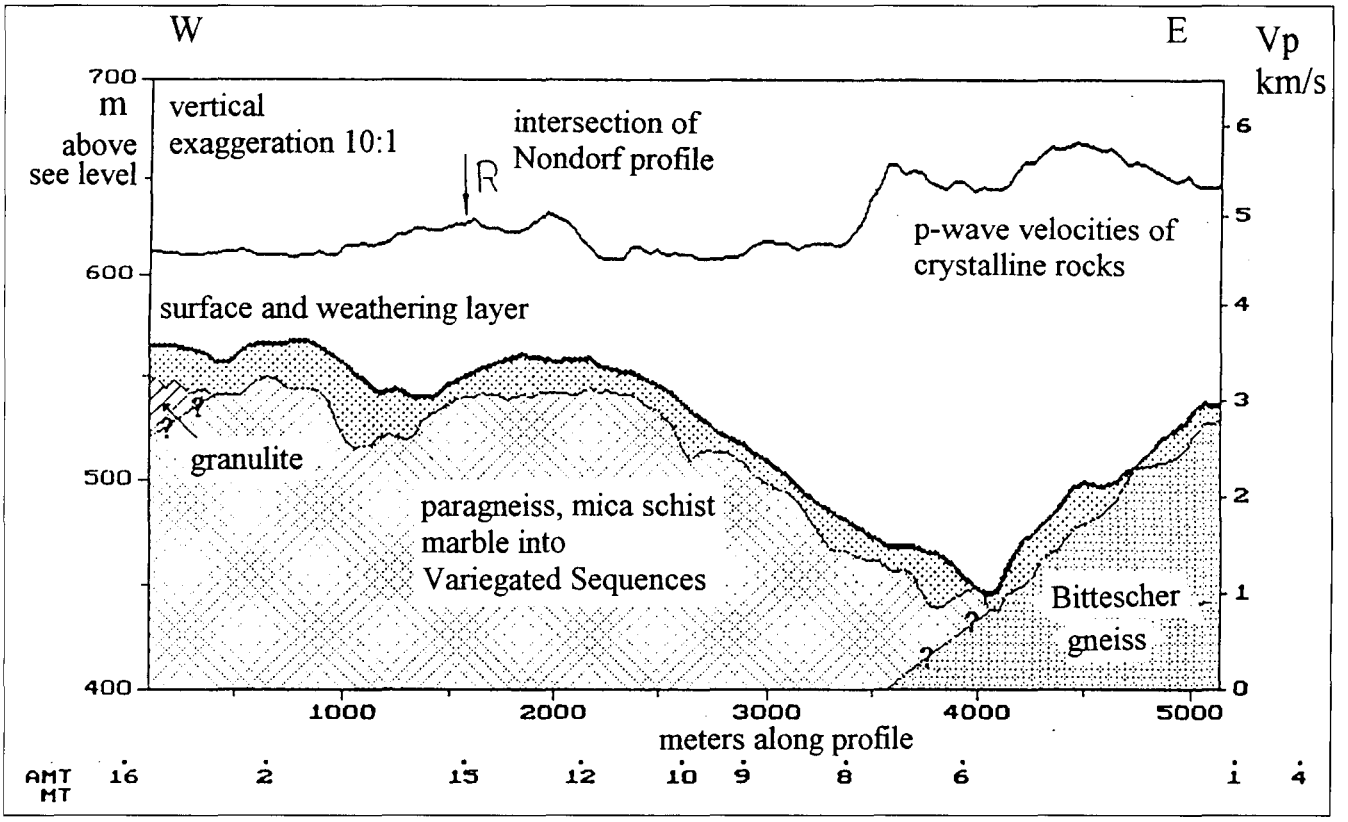

Text-Fig. 4.
Nondorf refraction seismic profile: topography, thickness of Quaternary sediments, P-wave velocity of the crystalline rocks.
R: intersection of Messern profile.

small energy (weight drop) seismic information is confined to the upper most 100 m of the bedrock. The most significant result (Text-Figs. 3 and 4) is a remarkable V_p-velocity contrast between Bittescher gneiss (5.4 ± 0.1 km/s) and Variegated Sequence (4.6 ± 0.1 km/s). Local variations of V_p are not as significant in comparison to the marked velocity contrast of these two units. It is displaced towards the South by 250 m (profile Nondorf) and towards the West by 350 m (profile Messern) from the surface outcrop of the contact zone between Bittescher gneiss and Variegated Sequence. Two explanations are possible:

- The Variegated Sequence overthrusts the Bittescher gneiss, where the boundary below profile Nondorf dips steeper than below the Messern profile.
- The acoustical parameters of the contact zones are comparable with those of the Bittescher gneiss. This might be due to intercalated marble lenses.

In general, lateral V_p-variations correlate quite well with boundaries of paragneisses, marbles and schist mapped in this area. The granulites and the Variegated Sequence rocks however seem indistinguishable at the surface. This can be observed on the Messern profile (see also event C in Text-Fig. 5). On the other hand the velocity of the granulites is much lower than that of the Bittescher gneiss. Therefore significant differences of their petrographical properties are probable.

Static corrections were derived from refraction seismic measurements (10 m geophone spacing after CGP-sorting). The reduction level has been selected at 540 m above mean sea level. All traces of the CMP-sections have been bandpass filtered (60–130 Hz). In addition a 50 Hz notch filter was applied to delete the mains pickup at the western end of the profile. Constant stacking velocities varied from 4.6 km/s to 5.6 km/s by steps of 0.1 km/s. 5.5 km/s appeared as the best value. This velocity has been used in CMP-stacking of both profiles. The coverage was 12-fold in most cases (Text-Figs. 5 and 6). The CMP-sections were interpreted as two way travel time (TWT) sections of normal incident waves. Maximum spectral seismic energy occurs with frequencies of about 80 Hz. Hence, at a velocity of 5.5 km/s the wavelength is about 70 m, and a vertical resolution of 20 m follows. In this region not enough rock samples are available for density measurements. Therefore significant density contrasts, which would lead to a great reflection coefficient, would occur at shear and mylonite fault zones (see A and C in Text-Fig. 6). If the observed large velocity contrast between Bittescher gneiss and Variegated Sequence continues to greater depths strong reflections at the common boundary would be expected. The reflection coefficient between granulites and Variegated Sequence is expected to be low, but the brute stack shows strong events (C in Text-Fig. 6). However, the reflection seismic data from tectonic crystalline rocks are often characterised by low signal to noise ratios and inconsistent reflection events (see also KIM et al., 1994).

2.2. Reflection Profile Messern

The profile of Messern-Rotweinsdorf has a length of 5 km. It starts within the granulite of St. Leonhard in the West and runs across the Variegated Sequence into the Bittescher gneiss unit in the East. It runs almost perpendicularly to the general strike of the geological units, especially of the Bittescher gneiss (Text-Fig. 2). The interpretation has to be performed with care because of the expected steep inclination of reflecting elements. The top part of this section (100 ms) is sensitive to the chosen

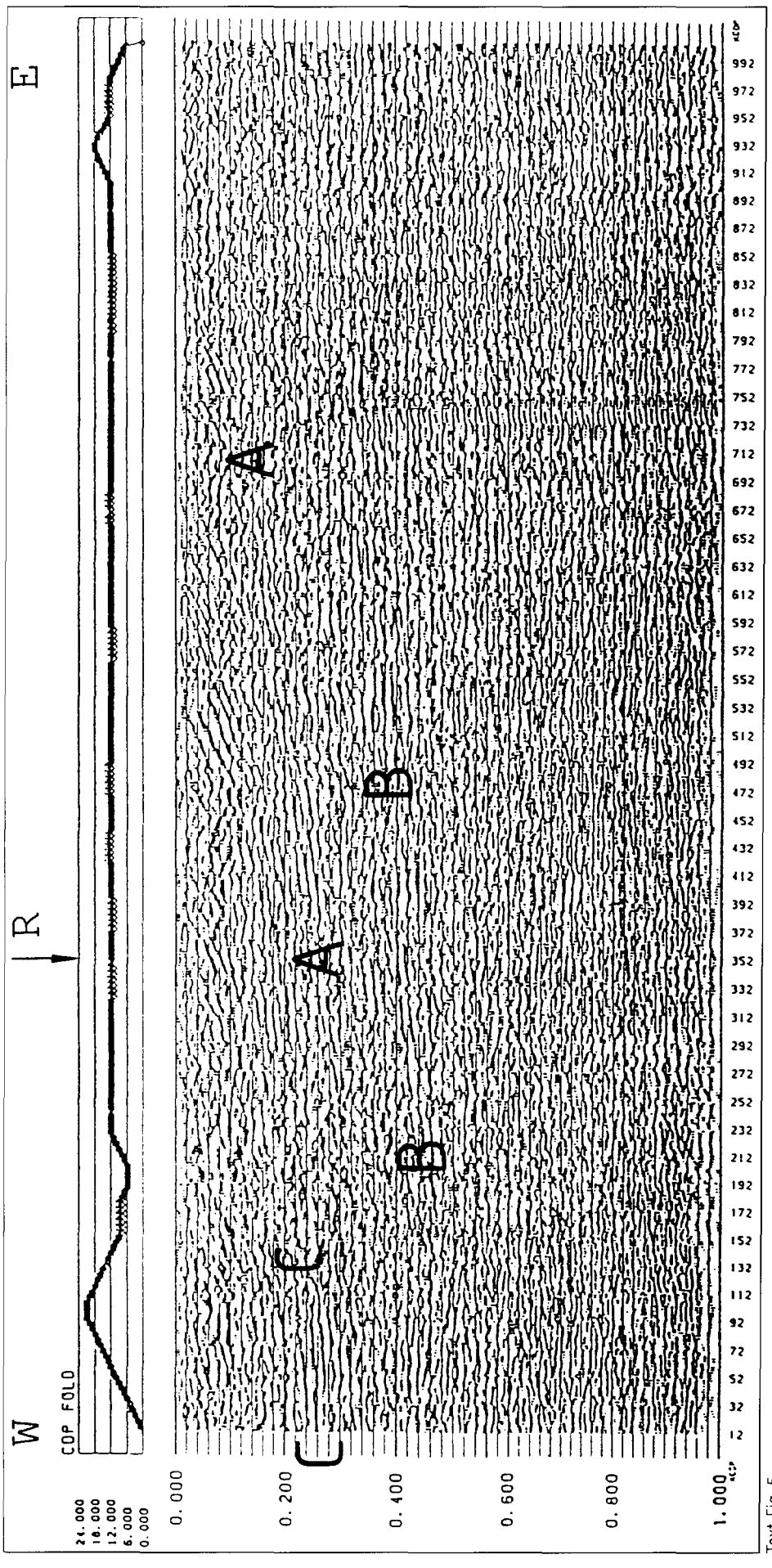

Text-Fig. 5.
Final brute stack of Messern profile.
Abscissa: CMPs, CMP-interval = 5 m; ordinate: two-way-travel time [s]; A, B, C = events; R = intersection of Nondorf profile.
Top: graph of the CMP fold.

stacking velocity and to the static corrections applied. At greater depth the assumed velocity is less critical. A constant velocity of V_p = 5.5 km/s has been used. NMO-corrected gathers were inspected to see whether there is an influence of first breaks. A 30 % to 50 % stretch mute has been tried, the latter being preferred. This mutes out that portion of any traces which has been NMO-stretched. It offers a way of removing first breaks automatically.

In addition to the stretch mute a compromise single front-end mute was applied to ensure that first breaks were completely removed.

The resulting brute stack (Text-Fig. 5) shows real events to a depth of 460 ms at the western end. Additionally the shallow events between CMPs No. 470 and 600 have been double checked on CMP gathers to distinguish them from artificial effects. Additionally a Stolt FK migration with 5.5 km/s velocity was carried out with results comparable to those shown in Text-Fig. 5.

The finite difference depth migration using the same velocity of 5.5 km/s (Text-Fig. 6) shows some good reflectors dipping smoothly to West from 0.4 to 0.6 km (event A) and from 1.1 km to 1.2 km depth in the middle of the section (event B). The seismic signals at the eastern end at 0.4 to 0.6 km depth (event C) are also reflections (probably a mylonite zone between granulites and Variegated Sequence).

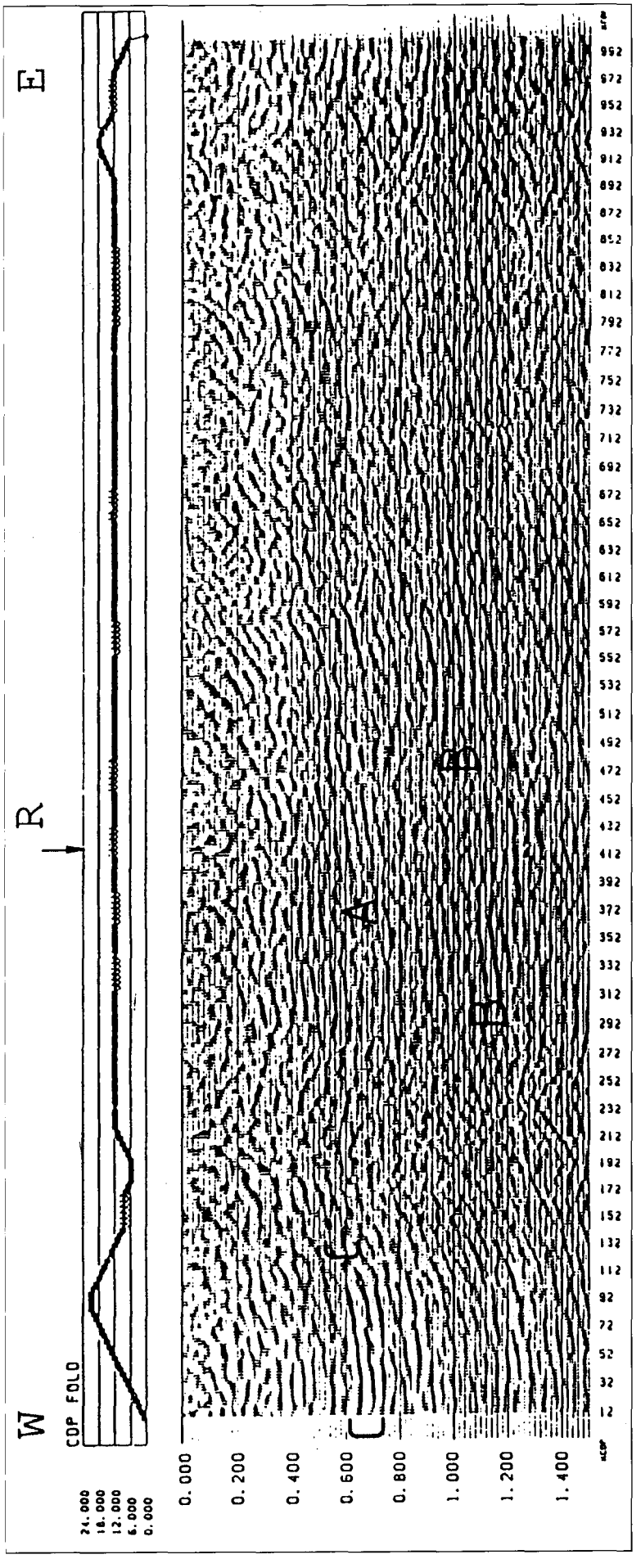

Text-Fig. 6.
Finite difference migration of Messern profile.
Migration velocity 5500 m/s = const.
Abscissa: CMP-number, CMP-distance = 5 m; ordinate: depth [m]; A, B, C = events; R = intersection of Nondorf profile.
Top: graph of the CMP fold.

2.3. Reflection Profile Nondorf

The profile Nondorf – Dietmannsdorf (length 3.5 km) begins in the North in the Bittescher gneiss and terminates in the Variegated Sequence. Below this profile the strike of the geological units is not well known (Text-Fig. 2). The static corrections compromise mutes and the brute stacks have been performed in a similar way as on the profile Messern. On the final brute stack (Text-Fig. 7), the reflectors are rather horizontal. The finite difference depth migration (Text-Fig. 8) shows these events rather clearly. Additionally, in the central part of the profile (CMP 262) a peak is visible. Between CMPs 372 (intersection point R) and 22 a strong reflector appears at a depth of 0.6 km (event A). Further short but strong reflecting elements occur in a depth range between 1 and 1.2 km. The pattern of reflecting elements is vague. The reflected waves are suspected to belong to different incident planes, including out-of-plane reflections. Therefore the common interpretation of these profiles is not easy (Text-Figs. 2, 5 and 7). However, in both cases at the intersection point R reflectors at 0.5, 0.9 and 1.1 km depth are observed (events A and B). Details of the seismic processing of the Nondorf and Messern profiles are given by SMYTHE (1994)

2.4. Deep Seismic Measurements

Deep structures of the lithosphere below the SBM are discussed in this part. Older concepts regard the crystalline of the Bohemian Massif as a medium with acoustical properties varying within narrow limits. Therefore it was suspected that reflection seismics is of limited use. However, recent reflection seismic studies proved strong seismic reflections originating in this depth range (TOMEK et al., 1987; TOMEK et al., 1993; BITTNER & WEVER, 1991; MEISSNER and the DEKORP RESEARCH GROUP, 1991). These observations indicate the existence of detailed structures in the upper and lower crust. Therefore they have been taken as an encouragement for the application of different seismic methods.

First a pilot project along a 5 km profile has been performed using

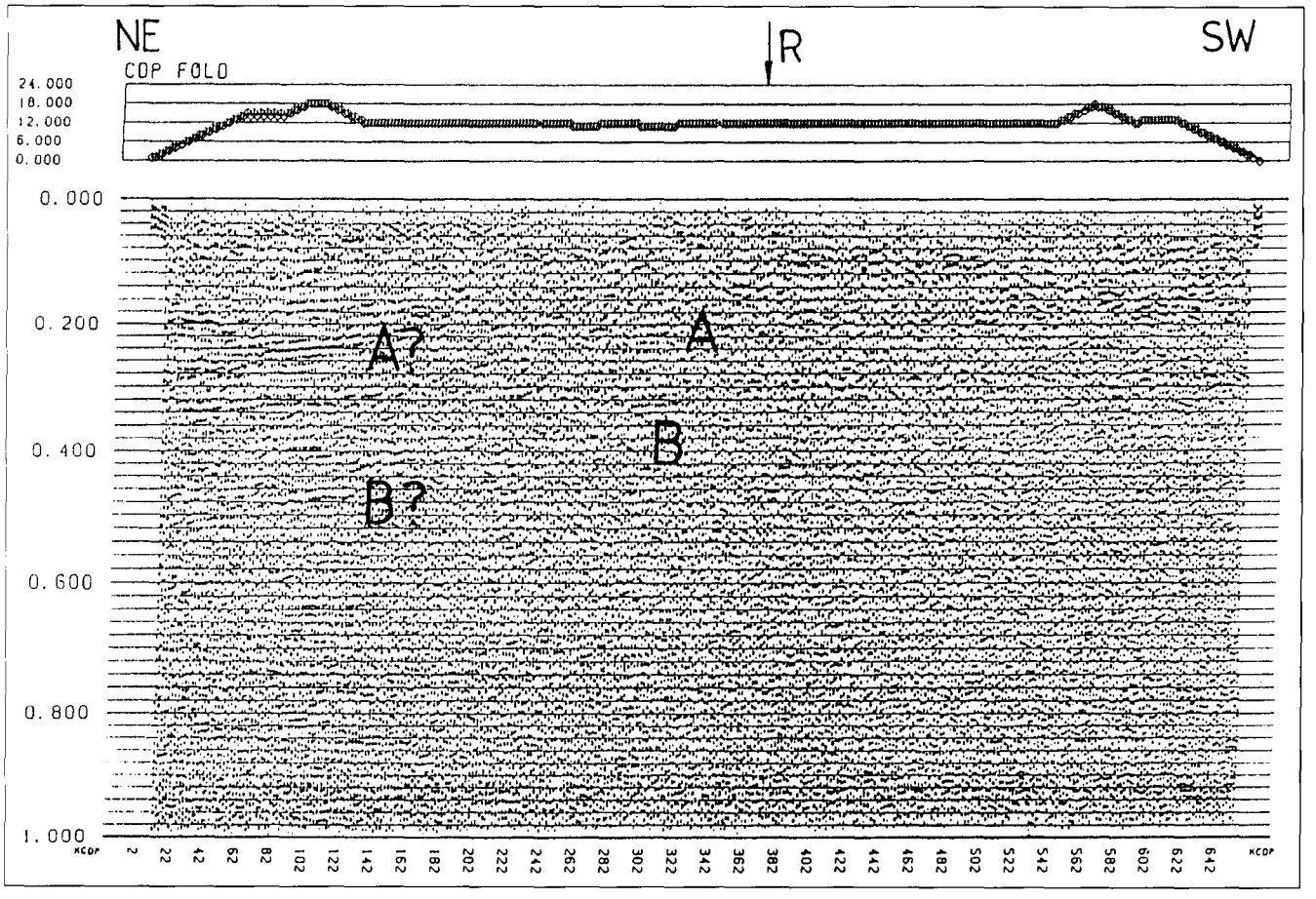

Text-Fig. 7.
Final brute stack of Nondorf profile.
Abscissa: CMP-number, CMP-distance = 5 m; ordinate: two-way-travel time [s]; A, B, C = events; R = intersection of Messern profile.
Top: graph of the CMP fold.

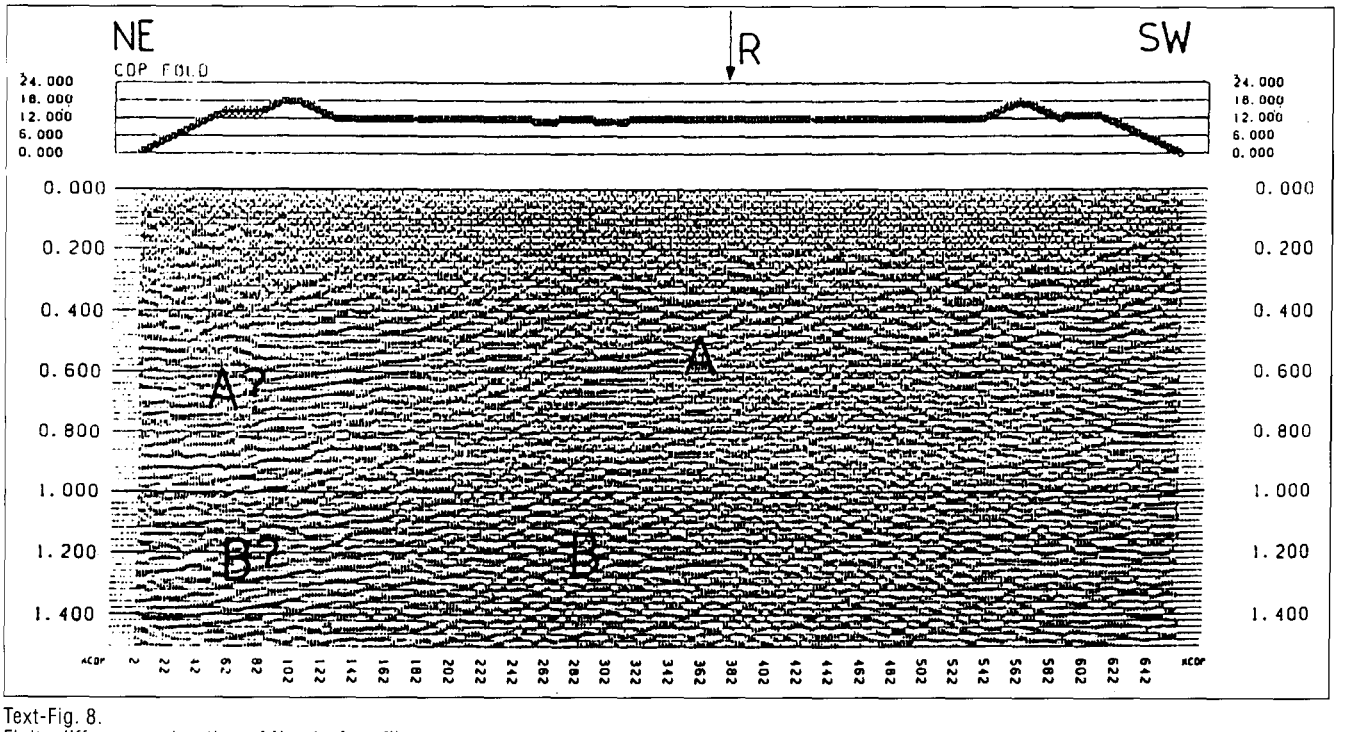

Text-Fig. 8.
Finite difference migration of Nondorf profile.
Migration velocity 5500 m/s = const.
Abscissa: CMP-number, CMP-distance = 5 m; ordinate = depth [m]; A, B, C = events; R = intersection of Messern profile.
Top: graph of the CMP fold.

shooting in a deep well near St. Martin (SW of Gmünd, see Text-Fig. 1). These measurements were performed in co-operation with the Institute of Geophysics of the Mining University of Leoben. It was planned as a pilot program to examine whether deep seismic reflections of high quality can be obtained in an area with crystalline rocks like in the Bohemian massif. A 4750 m long reflection seismic profile near St. Martin Southwest of Gmünd was carried out in Hercynian granite (Text-Fig. 1). The spacing of geophone groups with 12 geophones was 50 m. Two SERCEL-devices (338 HR) each with 48 channels were combined. Three single shots in a deep bore hole have been recorded with a high pass filter (125 Hz) and with a sampling interval of 1 ms.

First the V_p-velocity of the upper parts of the granite intrusion has been determined by bore hole velocity measurements down to a depth of 300 m. It increases from 830 m/s to 5580 m/s between surface and a depth of 19 m, and then remains nearly constant (V_p = 5580 ± 45 m/s). A shot in 125 m depth (50 kg special seismic TNT) generated reflections with good quality. Values of V_p = 5500 m/s, V_s = 3270 m/s and surface wave velocity of 2690 m/s are observed near surface. Reflections from elements in the upper crust with travel times of normal incident P-waves less than 5 s TWT are rare and poor. This result indicates a rather homogeneous velocity structure down to a depth of approximately 10 km. Later short reflection elements appear. At 8.2 s TWT the first reflection signal with considerable energy emerges. A wide band of reflected wave groups occurs between 10.3 and 11.5 s TWT which probably reflects the M-discontinuity. Using the mean V_p of 6.1 km/s taken from the observation of distant earthquakes at the station of Zwettl (see below) the depth of the M-discontinuity can be estimated at a depth of 31 km. This mean value of V_p in the crust is well established by several measurements (BARTELSEN et al., 1982; DEKORP RESEARCH GROUP, 1985; 1988). STRÖSSENREUTHER (1982) found similar values by reflection and refraction seismics at the southern margin of the Bohemian Massif. Even results of distant seismic profiles confirm this value (MEISSNER and the DEKORP RESEARCH GROUP, 1991).

Remarkable bands of reflections from the lower crust and the lack of reflections from the upper crust seem to exist in different areas of the Bohemian Massif (MEISSNER et al., 1982, 1984). The DEKORP profile D2S (Bavarian Moldanubian) shows clustering of reflection elements between 5 and 10 s TWT. Here, the crust with poor reflections reaches down to 25 km.

3. Magnetotelluric and Audiomagnetotelluric Soundings

The results of seismic measurements show a clustering of related and unrelated short reflecting elements below the profiles. They only partly reflect the geological features. Preferably completely different methods have to be applied. Therefore magnetotelluric (MT) and audio magnetotelluric (AMT) measurements have been performed. These methods help to understand the electrical properties of the underground like the resistivity of the layer structure, which is an important parameter for the geological interpretation of the profiles (e.g. CAGNIARD, 1953). They use the local deformations of the horizontal components of the natural electromagnetic fields of long periods T > 1 s (MT) and short periods T < 1 s (ATM). The MT and AMT measurements have been carried out on 13 sites located on the profile of Messern (Text-Fig. 2). Electrical and acoustical data obtained from the same geological structure can be put in mutual relation and lead to an interesting aspect of the interpretation. The field work has been performed in co-operation with the Geodetical and Geophysical Institute of the Hungarian Academy of Sciences in Sopron.

Additionally the ratio of the variations of the vertical to horizontal magnetic components, i.e. the induction arrows allow a general test of the lateral variations of the electrical resistivity. The arrows (C_r = real part), calculated from the AMT measurements at a constant period of 7.3 and 41 Hz should be directed to the area of smaller electrical resistivity (PARKINSON, 1962). This rule holds for many but not for every case. The length of the arrow is proportional to the variation of the ratio of the vertical to the horizontal components of the magnetic field, which theoretically should vanish in horizontally layered media. Therefore the arrow acts as an indicator of lateral inhomogeneities of the electrical parameters. Text-Fig. 2 shows that the induction arrows at the western sites No. 8, 9, 10, 12, 15, 17 and 18 in the Variegated Sequence are disturbed. There is a great degree of rotation in the direction of the vector between sites 8 and 9 and sites 17 and 18, the length of the arrows are also reduced. Here a phenomenon exists which has been observed in many cases by ARORA & ÁDÁM (1992) that the reduced vectors show the strike direction probably due to 3D effects inside the conductor. Site 6 differs considerably from the others because of the different electrical properties of the contact zone.

Because site No. 1 (Messern) in Bittescher gneiss and site No. 2 (Rotweinsdorf) in Variegated Sequence are nearly undisturbed, a standard program of 1-dimensional inversion (STEINER, 1989) of AMT and MT data for both sites has been applied for their extreme sounding curves (ρ_{max} and ρ_{min}) expressing the strong anisotropy of the metamorphic rocks. This evaluation leads to two simple distributions of the specific electrical resistivity (Table 1) where the maximum and minimum resistivity ρ_{max} and ρ_{min} only depend on depth. The model helps to obtain a general tendency of the electrical resistivity. Three important results have to be emphasised:

Table 1.
MT and AMT results.
H = layer thickness; ρ_{max}, ρ_{min} = maximum and minimum resistivity.

ATM + MT, site No.1 (Messern/E)			
$H(\rho_{max})$ [m]	ρ_{max} [Ωm]	$H(\rho_{min})$ [m]	ρ_{min} [Ωm]
8	13	3	4
1100	30540	1300	124700
14380	910	3890	12
-	> 10000	-	>10000
ATM + MT, site No.2 (Rotweinsdorf/W)			
$H(\rho_{max})$ [m]	ρ_{max} [Ωm]	$H(\rho_{min})$ [m]	ρ_{min} [Ωm]
7	2	400	9
270	3180	670	2
1660	15	2170	0.1
-	1020	-	> 10000

- In the western part of the profile both ρ_{max} and ρ_{min} are much lower than expected for dry crystalline rocks.
- There is some evidence of a high conductivity layer in a depth of some hundreds of meters below the profile.
- Both ρ_{max} and ρ_{min} are very much lower below site 2 than below site 1.

Remarkable differences between ρ_{max} and ρ_{min} indicate strong anisotropy as expected in layers with graphitoid or pyritic mineralization (e.g. ÁDÁM, 1987; ÁDÁM et al., 1990). Similar graphitic conductors have been indicated and studied in detail at the deep bore-hole KTB in Oberpfalz (Germany), which is located at the Western rim of the Bohemian Massif. Here it was stated that graphite (or carbon) has been accumulated along shear zones (ELEKTRB-GRUPPE, 1994).

3.1. Interpretation of AMT and MT Measurements by Complex Underground Models

A two-dimensional inversion has been carried out (Text-Figs. 9 and 10). The model makes clear that the high conducting layer has to be interpreted as Variegated Sequence. This formation is cut by Bittescher gneiss approximately at point No. 9. The Variegated Sequence overthrusts the Bittescher gneiss from West to East.

The two-dimensional inversion (Text-Figs. 9 and 10) shows a high conducting zone in the western part of the profile with a thickness in the range from 600 m to 1000 m and in distances from 1200 m to 3000 m (log $\rho_{max} = 1.5 \Rightarrow \rho_{max} = 31.6\ \Omega m$, log $\rho_{min} = 0.5 \Rightarrow \rho_{min} = 3.2\ \Omega m$). This zone is interpreted as Variegated Sequence. Between sites 2 and 8 outcropping graphite or/and pyritic accumulations are expected (FUCHS & MATURA, 1980; SCHRAUDER et al., 1993). The zone of low conductivity in the East is due to Bittescher gneiss, which dips under the Variegated Sequence from East to West ($2.5 \leq \log \rho_{max} \leq 3.5$, $\log \rho_{min} \cong 1.5$) as can be seen in the isoline plot of Text-Figs. 9 and 10. There is some evidence of an additional inversion layer below Bittescher gneiss in the eastern part in depths above 800 m (at 5.5 km, $1.5 \leq \log \rho_{min} \leq 3.5$). In this area phyllites and mica schists dipping to the W are observed (see also Text-Fig. 11). Further to the West between points 0 and 900 m of the profile there exists also a contrast between granulites and the Variegated Sequence with $\log \rho_{max} = 2 (\Rightarrow \rho_{max} = 100\ \Omega m)$, $\log \rho_{min} = 1 \Rightarrow \rho_{min} = 10\ \Omega m$).

3.2. Common Interpretation of Seismic, MT and AMT Measurements

The results of both AMT and seismic measurements correlate with geological and tectonic features in the area of Rotweinsdorf – Messern (ARIC et al., 1997). Because of the different accuracy and physical significance of the seismic and the AMT models a joint interpretation can be given with some restrictions. Text-Fig. 11 shows a best fitting model according to the geological, seismic and magnetotelluric data. The interpretation is based on Text-Figs. 6 and 9. The Bittescher gneiss forms an extended flat body here. The upper seismic horizon has high reflectivity due to the V_p-velocity contrast between 4.5 km/s to 5.5 km/s separating the Bittescher gneiss from the Variegated Sequence (seismic event A). This has been observed at a depth of 600 m at the intersection point R of both profiles (Text-Figs. 6 and 8). The Variegated Sequence below the granulites is linked by a conductivity inversion with $0.5 \leq \log \rho_{min} \leq 1$ from 0.8 to 3.8 km West of event A. The lower seismic event is interpreted as boundary to the Bittescher gneiss separating phyllitic mica schists and paragneisses (event B at 1.2 km depth). Because the para-

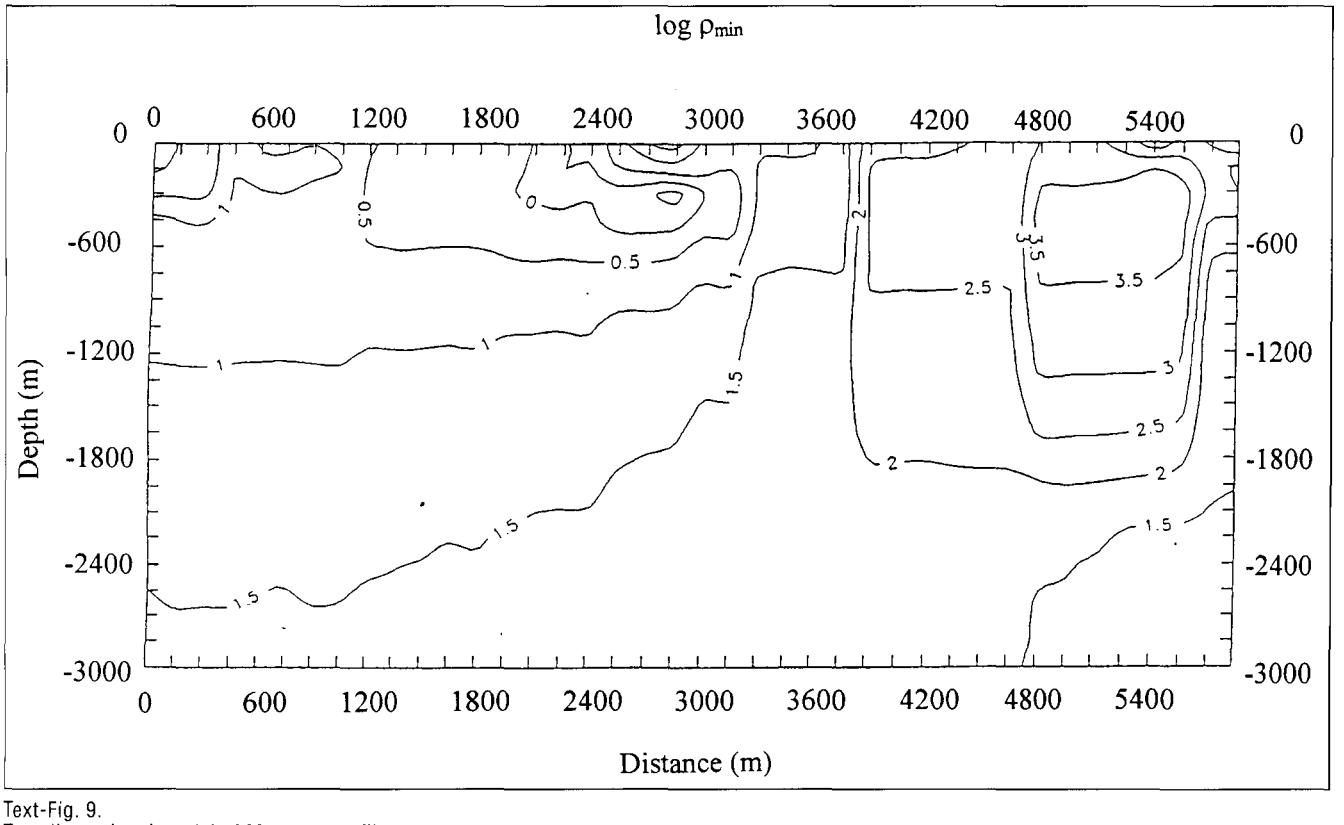

Text-Fig. 9.
Two dimensional model of Messern profile.
$\log(\rho_{min}\ [\Omega m])$ as function of distance [m] and depth [m]. Isolines: $\log(\rho_{min})$.

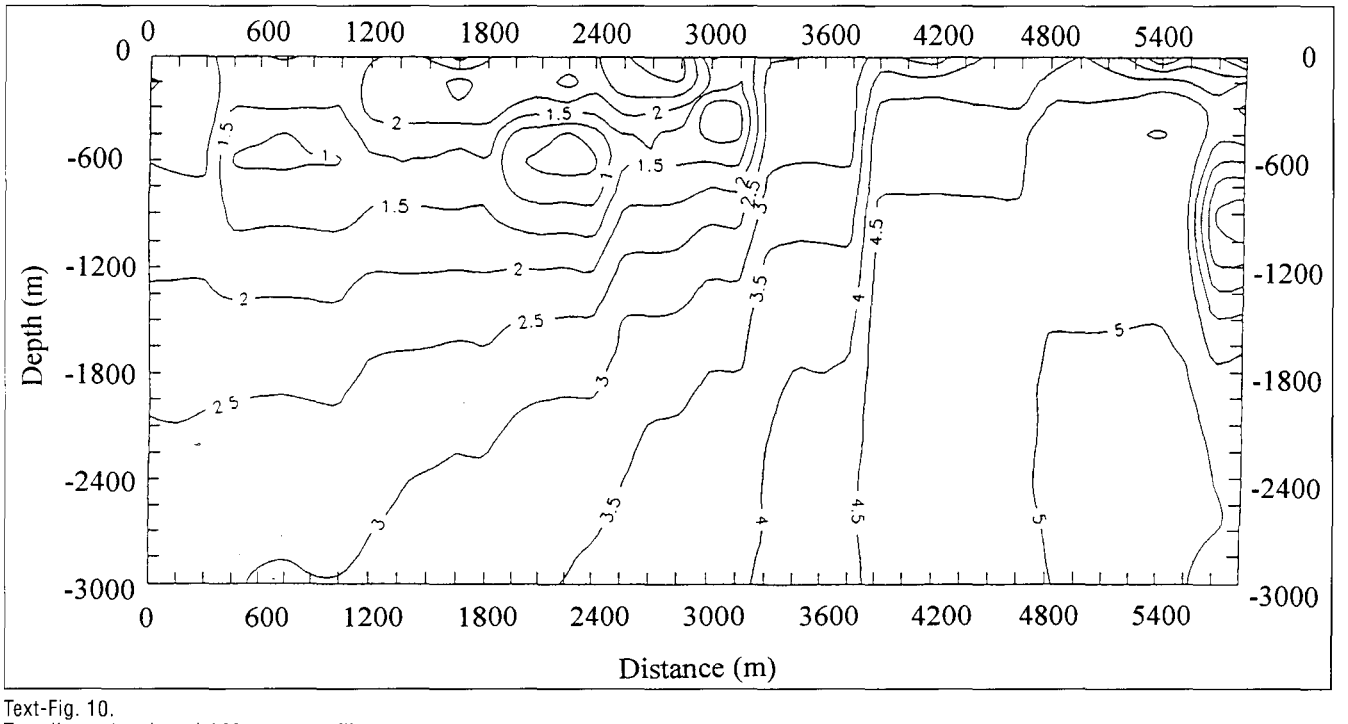

Text-Fig. 10.
Two dimensional model Messern profile.
$\log(\rho_{max}\,[\Omega m])$ as function of distance [m] and depth [m]. Isolines: $\log(\rho_{max})$.

gneisses are similar to those of the Variegated Sequence, the reflectivity of event B could be in the same range of magnitude as that of event A. This conclusion is not yet verified by seismic measurements directly on phyllitic mica shists and paragneisses. These units are exposed close to the Thaya batholite in the East. The AMT measurements however show this inversion rather clearly (see $1.5 \leq \log \rho_{min} \leq 2.0$ at distances of 4.2 km to 5.4 km, Text-Fig. 11). Both methods (seismics and AMT) give evidence of the dip of the Variegated Sequence below the granulite in the western part of the profile (event C). The depth of the events A and B seems to correlate with respective electrical resistivity isolines. There is no sign at all of any westwards emerging events or resistivity isolines. Contrary the results show only structures gently dipping to the West. The shallow steep reflection elements can be associated with overthrust structures and fault planes between rocks of different physical properties (Text-Fig. 11). FRITZ (1991)

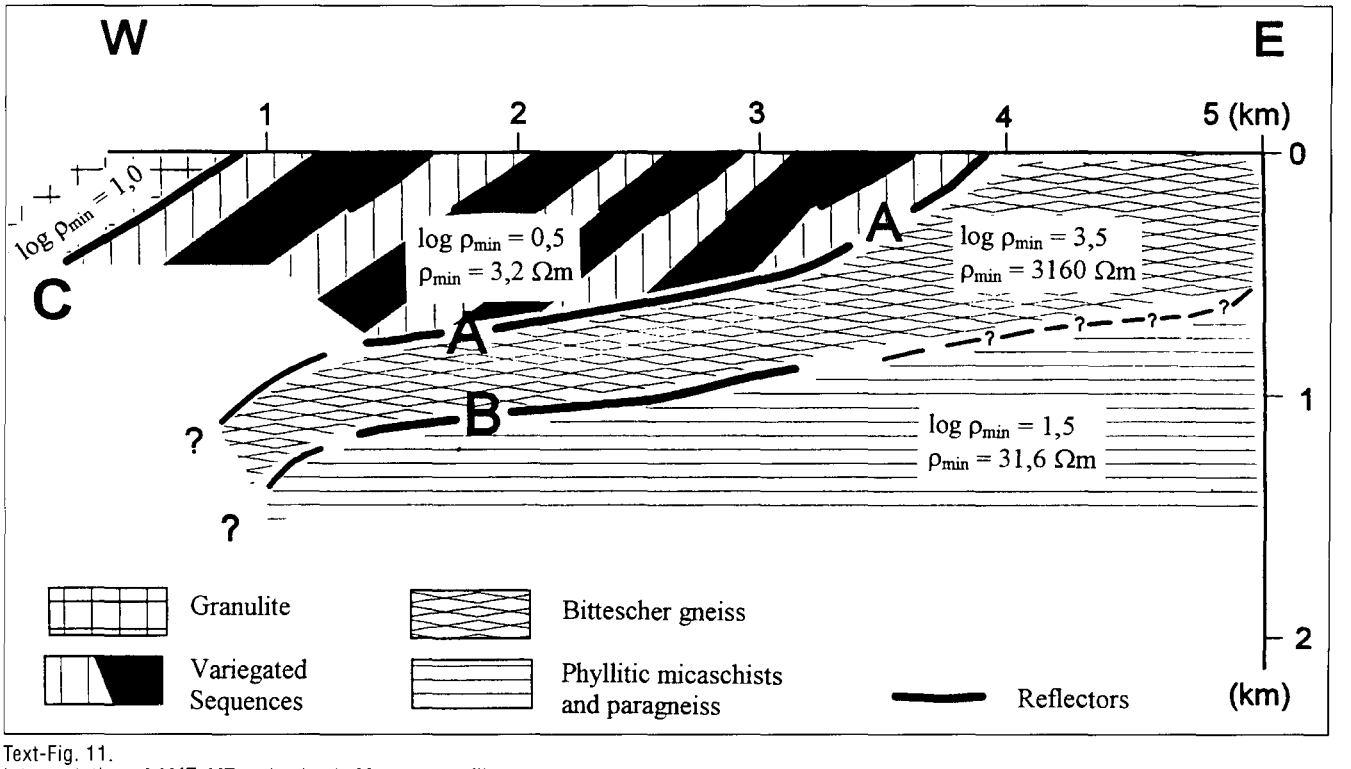

Text-Fig. 11.
Interpretation of AMT, MT and seismic Messern profile.
A, B, C = events (see also Figs 5–10 and Table 1).

Table 2.
Selected earthquakes.
Focal parameters taken from the "Regional catalogue of earthquakes, ICE 1988–1991".
M = magnitude, h = focal depth, Δ = epicentre distance, i_0 = angle of incidence (P-waves) at the Moho in the Eastern Alpine area.

location	date	coordinates		M	h	Δ [°]	i_0 [°]
		[°] N	[°] E				
KYUSHU	87-03-18	32.0	131.8	6.4	54	81	10.2
ANDREA	87-05-06	51.3	180.1	6.3	20	80	10.6
ICELAND	87-05-25	63.9	340.3	5.8	8	25	19.0
MID.ATL.RIDGE	88-04-20	1.0	330.0	5.8	10	60	13.7
TONGA	89-01-01	-18.5	185.4	6.0	123	149	3.2
W-BRASIL	89-05-05	-8.2	288.6	6.4	604	93	11.0
SAKHAL	90-08-20	46.2	142.2	5.9	301	75	11.4

and FRITZ & NEUBAUER (1993) have interpreted the deformation in terms of East-vergent folds and overthrusts formed in a stress regime with a maximum compressive stress direction aligned E–W.

4. Crustal Models Derived from Teleseismic Events

Mainly P- and S-waves from earthquakes observed at the seismological network in the Eastern Alps and the Bohemian Massif have been analysed. Seismograms of the three-component station in Zwettl were available to obtain information about the lower crust. Additionally recordings of 6 other stations of the Eastern Alpine seismic network have been used. All instruments show a constant velocity transfer function (vertical component) between the 0.1 and 5 s period (GUTDEUTSCH & ARIC, 1976). In this study the transmission function of a horizontally layered medium with arbitrary distribution of elastic parameters (e.g. FUCHS, 1968) has been calculated using the z-transformation (TREITEL & ROBINSON, 1966). This calculation leads directly to the impulse response of the medium. The comparison of synthetic and experimental seismograms allows the determination of crustal models.

In the first step crustal models disregarding converted S-waves were tested. According to the average crustal thickness and the mean V_p-velocity of the Eastern Alpine crust (ARIC et al., 1989; 1992; 1993) one can expect crustal reflections in a more confined time window of 3–14 s after the first break. Unfortunately in many seismograms this window includes disturbing signals like pP, sP, PcP and core phases. Therefore, before interpretation, seismograms are sorted into suited epicentre distances $70° \leq \Delta \leq 125°$, $158° \leq \Delta \leq 180°$ and focal depths. After inspection of about 500 seismograms the following events have been selected (Table 2).

First the simple model of a homogeneous crust with thickness H and velocity V_p has been calculated (JERAM, 1992). A synthetic seismogram has been adjusted to the seismogram observed at the station of Mariazell (MZA). The event occurred on the Middle Atlantic Ridge at 20 April 1988. The phases pP and sP have been registered as well as several additional phases PP and PPP, which are due to multiple reflections. The angle of incidence at the mantle-crust boundary has been calculated according to the Jeffrey-Bullen tables. These phases are the input signal which gives the theoretical seismogram after convolution with the impulse response of the layered crust. This method has been applied for all earthquakes listed in Table 2. The resulting crustal models were averaged. The results are listed in Table 3. Because of the well known inhomogeneous structure of the Alpine crust (POSGAY et al., 1991; ARIC et al., 1989; 1992; 1993) the depth accuracy is about 1 km.

In a next step the influence of converted shear waves has been studied. The horizontal component contains important information about the P- to S-conversion and therefore helps to find more confined models of the crustal structure (Text-Fig. 12; CHWATAL, 1993). Earthquakes in epicentre distances of $30° \leq \Delta \leq 70°$ provide optimal conditions for undisturbed registrations. Some of the studied earthquakes are shown in Table 4.

The resulting horizontal component was derived from the EW and NS component. The comparison of observed and synthetic seismograms has been carried out in the same way as described before. The best fitting one-layer model of the crust is shown in Text-Fig. 12.

Table 3.
Stations of the Eastern Alpine network (ARIC et al., 1992).
V_p = averaged velocity of the crust, H = Moho-depth; V_p = velocity of the upper mantle = 8.2 km/s.

station	site	latitude [°]	longitude [°]	elevation [m]	V_p [km/s]	H [km]
BBA	Bleiberg	46.79	13.70	887	6.2	41
BGA	Bad Gleichenberg	46.88	15.91	320	6.2	33
GHA	Glashütten	47.38	16.39	500	6.2	36
HSA	Hoher Sonnblick	47.05	12.96	3100	6.2	47
MZA	Mariazell	47.77	15.33	990	6.2	33
KFA	Klagenfurt	46.63	14.29	480	6.2	45
PIA	Pitten	47.72	16.19	380	6.2	34
SZA	Zwettl	48.62	15.20	510	6.2	34

Table 4.
Selected earthquakes recorded at the station SZA (3 components).
Focal parameters taken from the "Regional catalogue of earthquakes, ICE 1988–1991".
M = magnitude, h = focal depth, Δ = epicentre distance, i_0 = angle of incidence (P-waves) at the mantle-crust boundary in the Eastern Alpine area.

Event	date	coordinates		M	h	Δ [°]	i_0 [°]
		[°] N	[°] E				
SIBIRIA	91-12-27	51.0	98.1	5.7	10	51	33
SEMLJA	92-02-17	79.2	124.5	5.5	10	46	35
COSTA RICA	92-03-07	10.2	275.7	6.3	73	89	20
N.-CALIF.	92-04-26	40.4	235.7	6.6	25	84	21
ALASKA	92-08-07	57.6	217.0	6.3	10	72	25

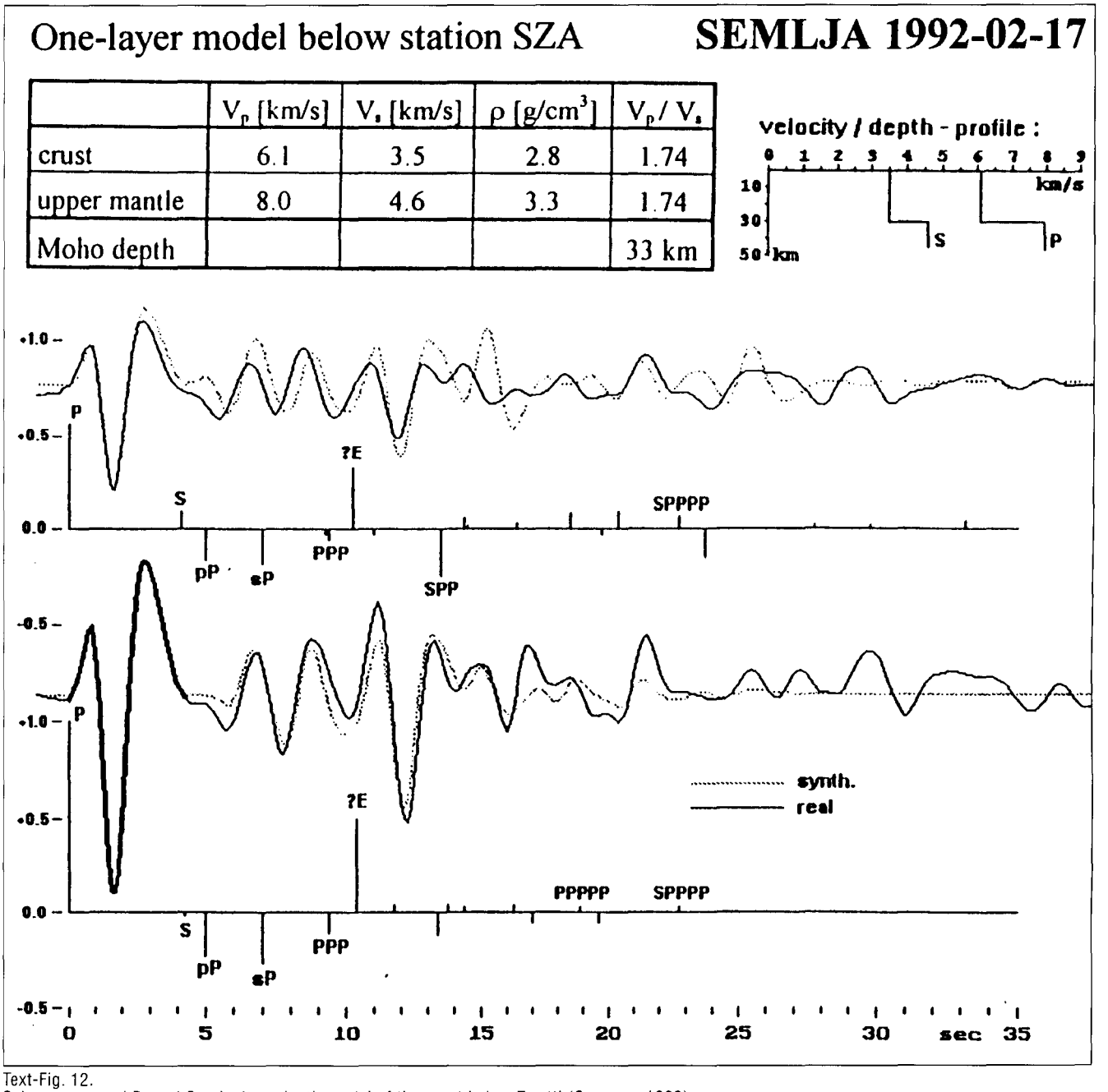

	V_p [km/s]	V_s [km/s]	ρ [g/cm³]	V_p / V_s
crust	6.1	3.5	2.8	1.74
upper mantle	8.0	4.6	3.3	1.74
Moho depth				33 km

Text-Fig. 12.
Seismogram and P- and S-velocity – depth model of the crust below Zwettl (CHWATAL, 1993).
Abscissa: travel time [s]; ordinate: relative amplitude.

5. The Bouguer Gravity

The resolution of existing gravity maps (SENFTL, 1965) is by far insufficient to obtain detailed information about upper crustal structures. Therefore a completely new gravity survey was performed resulting in about 5500 stations distributed regularly over the Bohemian Massif and the adjoining Molasse zone with a maximal station interval of 3 km (WALACH, 1990; MEURERS & STEINHAUSER, 1990; MEURERS et al., 1991). In some regions of local interest a

much higher station density was established. Text-Fig. 1 shows the station distribution. The Bouguer anomaly (Plate 1, top) was calculated using the following assumptions:

- Geodetic Reference System 1980 (MORITZ, 1980).
- Absolute gravity datum (RUESS, 1988).
- Second order approximation of normal gravity and free air reduction (WENZEL, 1985).
- Atmospheric corrections (WENZEL, 1985).
- Spherical mass correction up to 167 km radius (Hayford zone O_2) assuming a constant density of 2.67 gcm^{-3}. This value is close to the mean density of the surface rocks in the investigated area.
- Interpolation of a regular grid with grid spacing of 1 km by least squares prediction (KRAIGER, 1988) and bicubic spline representation (SÜNKEL, 1980).

A pronounced anomaly pattern of Bouguer gravity exists even in areas where low density sediments of the Molasse basin cover the crystalline rocks. Generally the margin of the Bohemian Massif is marked by a high gradient zone including several short wavelength anomalies due to rim synclines like near Eferding, Herzogenburg or Krems. Only in the western part of the map the regional trend of the Bouguer anomaly seems to be controlled by the gravity effect of the Mohorovicic-discontinuity. Within the eastern part upper crustal structures become increasingly dominant. The main tectonic units can be recognised in the gravity map. A distinct negative anomaly with an axis striking approximately N–S accompanies the South Bohemian granite pluton. A wide area with large horizontal gradients followed by a regional gravity high, which extends far into the foreland, characterises the transition to the metamorphic rocks adjoining in the East. Local anomalies of different signature superimpose this gravity high. At several locations there is a good coincidence with density provinces determined by analysing surface rock samples (MEURERS & STEINHAUSER, 1990). The Thaya pluton causes a negative anomaly striking NNE–SSW. This gravity low is followed in the East by a positive anomaly striking similarly. In this way a negative-positive anomaly couple is formed which completely covers the gravity effect of the Molasse sediments with increasing thickness towards the East. The basement structures cannot be observed before the Mailberg fault where the basement is dislocated vertically by several 100 m. Other local structures like the short wavelength gravity high near Hollabrunn are obviously due to basement undulations as confirmed by refraction seismic measurements. A high level Bouguer anomaly characterises the western part of the investigated area as well. Its amplitude however is much smaller than in the East. In the SW the anomaly pattern is typical for the Alpine situation where the effect of the crust-mantle boundary mainly controls the regional gravity. This effect is increased by the Molasse sediments thickening in the same direction as the crust in that area.

5.1. Gravity Map Stripping

The first interpretation step consists of estimating the magnitude of reduction anomalies due to assuming constant rock density for mass corrections. A high resolution model has been developed based on the digitised distribution of the surface rock density in Austria (STEINHAUSER et al., 1984a; WALACH, 1987). Detailed rock sample investigations performed in the terrain correction area (DUMA & JILG, 1991) were used for that purpose. A geographical grid system with a minimum grid spacing of about 370 m×390 m according to the height model applied for topography approximation defines the resulting digital density model. Its density provinces are resulting from statistical analysis of all available rock samples and digitisation (STROBL, 1993) of the geological map of the SBM (FUCHS & MATURA, 1976). Reduction anomalies of regional behaviour amount up to 5 mGal within the Molasse zone and to 1–3 mGal within the crystalline area. Therefore they have to be considered in quantitative interpretation.

For estimating the gravity effect of well-known crustal structures (crust-mantle boundary, Molasse sediments) the method of gravity map stripping was performed (MEURERS, 1991). Depth investigations of the Mohorovicic-discontinuity by seismic methods are known from the territory of the Czech Republic, Slovakia, Hungary and beneath the main crest of the Eastern Alps (POSGAY et al., 1991). A corresponding map of Southern Germany exists published by GIESE & PRODEHL (1986) which fits very well the results of POSGAY et al. In the area beneath the Austrian part of the Bohemian Massif the crust-mantle boundary model resulted from interpolating the digitised Moho depth data (MEURERS, 1990). It is confirmed by results of deep reflection seismics performed near St. Martin in the central region of the SBM and by P-, pP- and sP-wave travel time observations of distant earthquakes analysed for the station Zwettl (ARIC et al., 1993). The gravity effect of the crust-mantle boundary was calculated by applying the discrete Fourier transformation-method of PARKER (1972). A constant density contrast of 0.4 gcm^{-3} between lower crust and upper mantle material was assumed according to seismic results in that region. Plate 2 (top) shows the stripped Bouguer gravity map calculated by applying the digital density model and by subtracting the gravitational effect of the Moho undulation. A comparison with Plate 1 (top) reveals remarkable differences. This refers especially to the NNE–SSW striking gravity high in the West of Hollabrunn. Here, the anomaly diminishes by about 10 mGal compared to the gravity maximum due to the Raabs-unit (NW of Horn), which is dominated by amphibolites. That means the increase of the Bouguer gravity towards the East can partially be explained by the undulation of the crust-mantle boundary. In the Southwest the distinct gravity decrease from North to South continues. This is not only due to the thickening of the Molasse, but also to upper crustal structures in the crystalline which obviously cause the main part of all residual anomalies.

In a further step the gravity effect of the Molasse sediments was estimated in the eastern part of the investigated area. The calculations were based on the Tertiary basement depth map of the Molasse in Lower Austria compiled by BRIX et al. (1979). Incorporation of recent results obtained by seismic investigations and well logging (ROETZEL, 1989) improved this map at the margin of the Bohemian Massif. Reflection and refraction seismics were performed within the margin near Krems and Herzogenburg (STEINHAUSER et al., 1984b; 1985) respectively near Retz and Röschitz (STEINHAUSER et al., 1986; 1987). A density contrast of 0.3 and 0.4 gcm^{-3} respectively according to the digital density model has been applied (STROBL, 1993). Plate 2 (bottom) shows the resulting stripped gravity map. The high gradient zone connected with the Mailberg fault is completely removed proving the model to be suitable. The area of positive gravity along on the transition zone between the South-Bohemian granite intrusions and the metamorphic units of the Moldanubian is now extending far into the Molasse zone towards the East and Southeast. This indicates the existence of a deep crustal

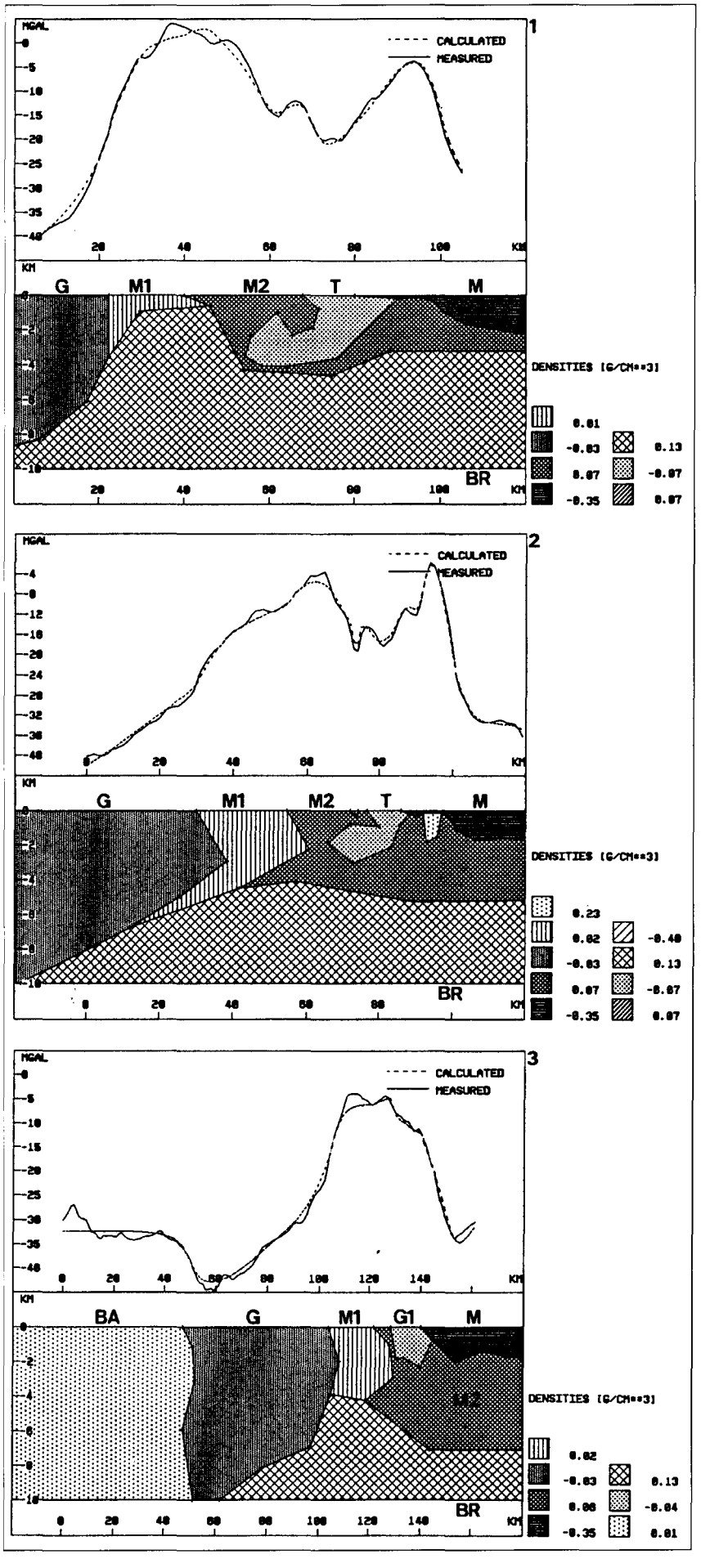

structure which begins at the eastern margin of the plutonian area and extends beyond the Mailberg fault.

5.2. Modelling

To develop a first view to the upper crustal structures two-dimensional modelling was performed (MEURERS, 1993) using an interactive graphical module based on the Talwani's algorithm (GOLTZ & SCHMIDT, 1992). Four profiles were selected, which cover the main tectonic units of the Bohemian massif and run approximately across the strike of the contour lines. They are marked in Plate 2 (top). The Bouguer gravity calculated with variable reduction density and stripped with respect to the Moho effect (Plate 2, top) serves as reference signal. Therefore all models can be restricted to upper crustal structures as long as no further information is available about the crust-mantle discontinuity and density structure within the lower crust. Boundaries defined by surface geology (FUCHS & MATURA, 1976) and the depth distribution of the Molasse basement (BRIX et al., 1979) are important geometrical constraints. Seismic investigations and several drillings within the marginal basins improved the latter as mentioned before (MEURERS et al., 1993).

Text-Figs. 13 and 14 show the two-dimensional modelling results. A common feature of all sections in Text-Fig. 13 is a high density crustal block, which begins at the eastern margin of the South Bohemian granite intrusion and extends far towards the East. In the present interpretation the upper crust in that region consists of the Brunovistulicum superimposed by partly metamorphic Moldanubian and Moravian units. Deep drilling at different locations on both sides of the Mailberg fault revealed several bedrock samples mostly consisting of high density (> 2.73 gcm^{-3}) gneisses or mica shists. This and the results of gravity map stripping support the general model conception. An alternative interpretation does not introduce the Brunovistulian crust. Instead of this the continuation of Moldanubian and Moravian metamorphic rocks extending both eastward and

Text-Fig. 13.
Two-dimensional model of the upper crust of the Southern Bohemian Massif.
Profiles 1–3 (marked in Plate 2, top).
BA = Bavaricum (2.68 gcm^{-3}); BR = Brunovistulicum (2.80 gcm^{-3}); G = Granite intrusion (2.64 gcm^{-3}); G1 = Granulite (2.63 gcm^{-3}); M = Molasse (2.32 gcm^{-3}); M1 = Moldanubicum (2.69 gcm^{-3}); M2 = Moldanubicum + Moravicum (2.74 gcm^{-3}); T = Thaya batholite (2.60 gcm^{-3}).

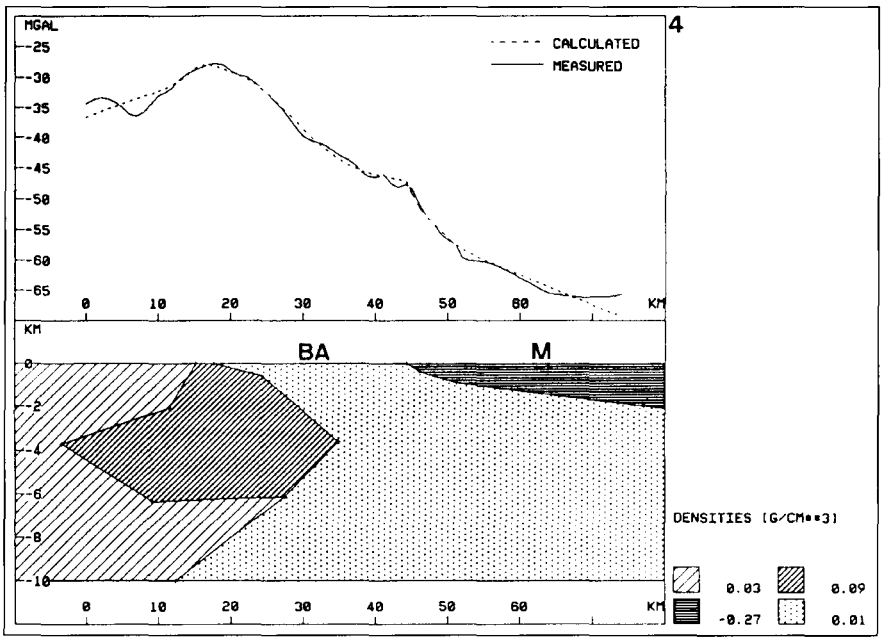

Text-Fig. 14.
Two-dimensional model of the upper crust of the Southern Bohemian Massif.
Profile 4 (marked in Plate 2, top).
BA = Bavaricum (2.68 gcm^{-3}); M = Molasse (2.40 gcm^{-3}).

below the Molasse basement is assumed. In both cases the lateral density contrast between the metamorphic units and the Thaya pluton (0.15 gcm^{-3}) or Molasse sediments (0.4 gcm^{-3}) respectively now explains the regional gravity high (H) between Retz and Hollabrunn. In that area the metamorphic part of the crust shows a vaulted structure. The local gravity high near Hollabrunn cannot be interpreted exclusively by the basement topography as determined by refraction seismics. To explain its amplitude the assumption of an additional high density source close to the surface is necessary. The same body perhaps contributes also to the pronounced local magnetic anomaly. The Thaya batholite increases from South to North concerning both horizontal and vertical dimensions. Shallow Molasse sediments cover the Thaya pluton in its eastern part. The eastward extension into the Molasse zone amounts to 2–4 km in the South (profile 2) and increases to about 10 km in the North (profile 1). The Thaya massif possibly extends southward to the Krems basin, the local gravity minimum of which can only be explained assuming additional low density sources within the crystalline basement (DANEU, 1993).

The eastern part of the SBM has been interpreted additionally by applying the interactive 3D-modelling method of GÖTZE & LAHMEYER (1988). The 3D-model confirms the regional features of the upper crust obtained by 2D-interpretation, but of course local structures (e.g. Molasse basement) are different (RADINGER, 1994). The local gravity high near Hollabrunn is here interpreted to be caused by a lens like source. This body is much deeper than the corresponding source of the 2D-model and therefore fits better to the magnetic modelling result (ARNDT, 1993).

The South Bohemian granite intrusion causes the regional gravity low in the centre region of the investigated area. Assuming a density contrast of about 0.1 gcm^{-3} in agreement with rock density investigations at the surface the intrusion extends down to a depth of about 10 km. This corresponds well to the results of density deconvolution (MEURERS & STROBL, 1993; STROBL, 1993) and of deep seismic sounding. The contact area between granite pluton and metamorphic rocks generally dips towards West. According to the horizontal Bouguer gravity gradient the dip angle decreases obviously from North to South. The western contact area can only be investigated on profile 3 as the northern profiles (1, 2) do not completely cover the granite intrusion.

Mean crustal density characterises the upper crust in the West of the South Bohemian granite intrusion. The gravity decrease from North to South observed in Plates 1 (top) and 2 (top) or profile 4 (Text-Fig. 14) can be explained completely neither by the steeply sloping Moho discontinuity nor by an increasing thickness of the Molasse sediments. Therefore a subsurface structure with high density contrast (0.09 gcm^{-3}) could be responsible for the positive anomaly in the NE although there is no geological evidence. This structure is possibly a subsurface continuation of the Variegated Sequence of Cesky Krumlov.

6. Magnetic and Radiometric Investigations

One of the main targets was to clarify certain structural and tectonic questions in the SBM which arose from magnetic and radiometric data. The SBM has been covered by aeromagnetic measurements in the late seventies and early eighties. The flight line spacing was 2 km; tie lines were flown with a distance of 10 km. In the mid-eighties in selected areas of the SBM complex aerogeophysical surveys, including aeroelectromagnetics, magnetics and gamma-ray spectrometry has been performed. The distance between flight lines was 200 m.

6.1. Magnetic Anomalies

The pattern of the magnetic anomalies (Plate 1, bottom) in the western part of the SBM, mainly controlled by large granitic intrusions, is characterised by a rather quiet signature. Partly it is interrupted by anomalies (HEINZ, 1991). The limited eastern part, mainly dominated by metamorphic rocks – including the rock sequences of the Moravian unit – shows numerous, mutual overlapping structures caused by magnetic sources situated in different depth ranges. The boundary between the plutonic and the metamorphic domain is marked clearly in the magnetic signature (Plate 1, bottom).

One of the major problems in interpreting magnetic anomalies in the SBM is the origin of the magnetic sources and their relationship to the general geological situation in this part of Austria. Frequently the magnetic structures occur along the margins of granitic intrusions. Quite often they correlate with alteration zones (e.g. Hirschenschlag, Nebelstein, Liebenau). According to these observations, it seems that those phenomena are due to complex and multiphase intrusion processes: younger intrusive bodies –

partly altered and mineralised – are in relation to the three major granitic events in the SBM (e.g. Nebelstein, Hirschenschlag). The highly mineralised "Homolka-granite", which lies on Czech territory, is represented on Austrian territory by quartzitic and porphyritic veins only. According to GÖD & KOLLER (1987), GÖD (1989) and KOLLER et al. (1992) these alterations are due to the influence of a biotite granite intrusion found in the course of a drilling program.

The sources of the magnetic anomalies are mainly secondarily formed magnetite crystals within limited altered zones. However, larger granitic complexes, like the "Karlstift-granite" are characterised by higher contents of secondarily formed magnetite as well. Using a portable susceptibility-meter it is possible even to distinguish a "standard" and an "anomalous type" of the Karlstift-granite (PRICHYSTAL, 1993; PRICHYSTAL & LOSOS, 1993). Typical mineral occurrences of secondarily formed magnetite are shown in Text-Fig. 15.

Near the village Liebenau the "Karlstift-granite" (definition according to KLOB [1970]) medium-grained, porphyritic biotite granite) intrudes into granitic bodies of "Weinsberg-type". Even along the contact zones of these granites magnetic anomalies could be observed. The Weinsberg-granite is characterised by low susceptibility values ($0.05–0.08 \cdot 10^{-3}$ [SI]), whereas over the Karlstift-granite higher values ($0.23–0.7 \cdot 10^{-3}$ [SI]) had been observed. Sometimes dark patches with even higher susceptibility values can be found in the Karlstift-granite. Also characteristic are magnetite pseudomorphoses after biotite. The magnetic anomalies near Liebenau are due to the altered contact zones of the Karlstift-granite, which had been influenced by the regional tectonic setting as well (Text-Fig. 16). Detailed model calculations indicate almost outcropping inclined magnetic bodies with bottom depths of approximately 1 km (HÜBL, 1993).

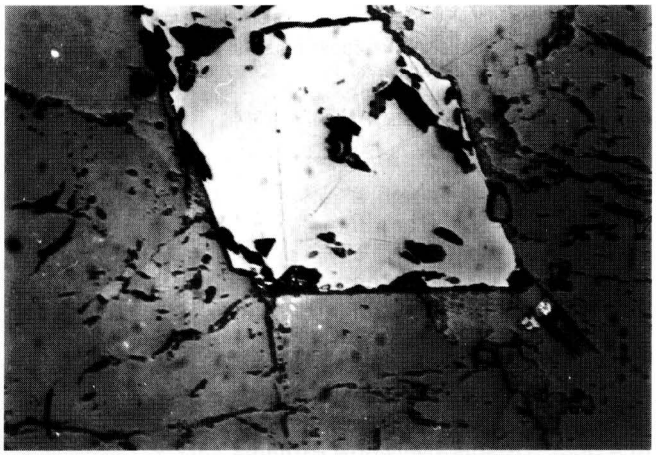

Text-Fig. 15.
Example of a subidiomorphic magnetite crystal (∅ 0.1 mm) from the Karlstift Granite.
The secondary forming process of the minerals is proved by frequent inclusions of rock forming minerals (PRICHYSTAL & LOSOS, 1993).

The magnetic anomaly pattern of the eastern and southern part of the SBM is mainly due to local and shallow sources (LIBOWITZKY, 1989; SEIBERL & HEINZ, 1990). In terms of geodynamics of this area a remarkable belt of magnetic anomalies, striking SSW–NNE, can be observed NE of the city of St. Pölten. This zone has been called "Dunkelstein Moldanubian Belt". It seems that it belongs neither completely to the Moldanubian nor to the Moravian rock sequences. This is supported also by other results (ARNDT, 1993). From detailed analyses of model calculations it appears as if at least the most southerly of these anomalies is not due to Moldanubian or Moravian rock sources.

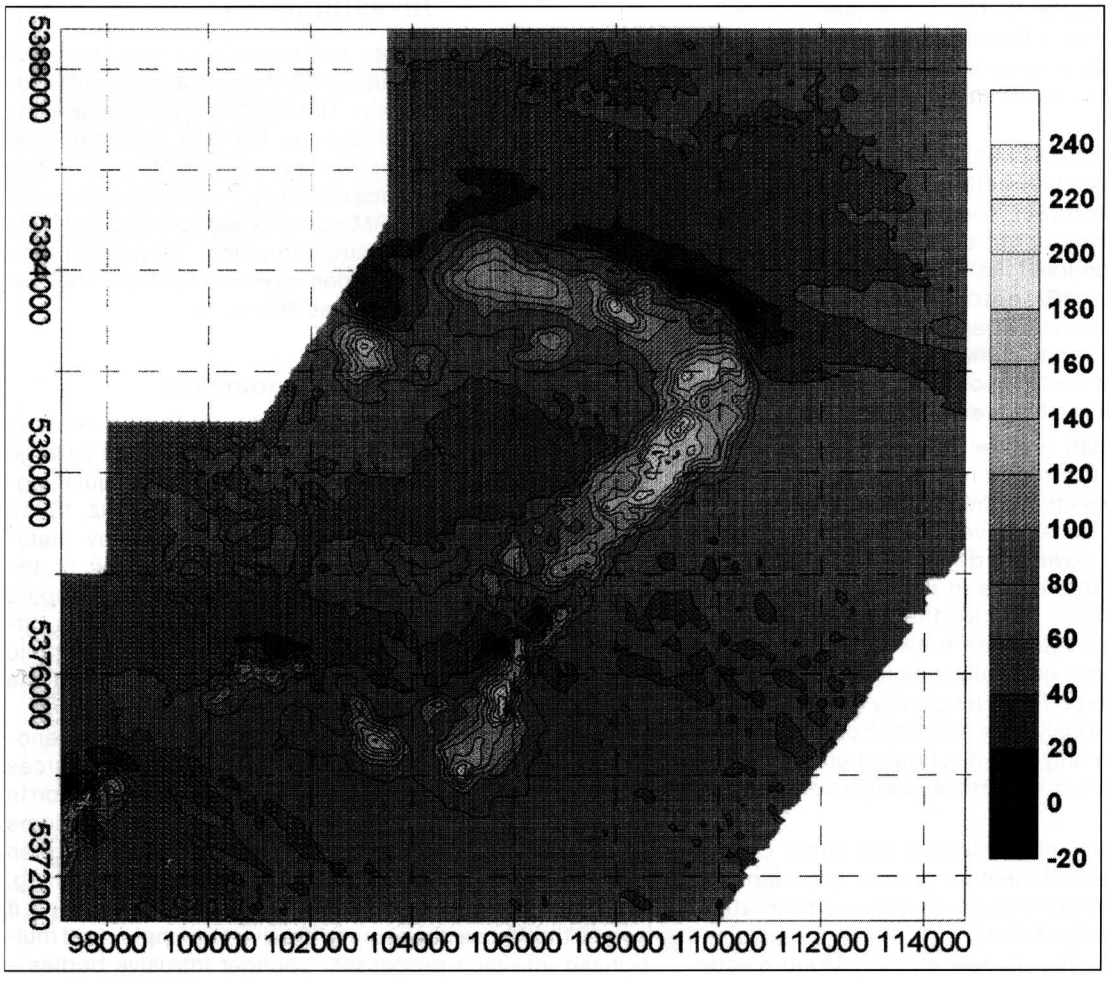

Text-Fig. 16.
The magnetic anomaly near Liebenau (HÜBL, 1993).
Isolines in [nT].

6.2. Radiometric Results

The mentioned alteration processes not only are accompanied by magnetite accumulations but also by anomalous distributions of natural radioactive elements, especially of Potassium (^{40}K). E.g. the central parts of the Karlstift-granite show rather low Potassium values, whereas the contact zones to the surrounding rocks are characterised by higher values. Most likely this Potassium distribution is due to leaching accumulative processes.

Comparable situations have been observed in the Nebelstein area (MOTSCHKA, 1995). In the western part of the large magnetic structure near St. Martin the U/Th-ratio distribution is anomalously high (>2,0) (see Text-Fig. 17). The more mobile Uranium-minerals have been accumulated in comparison to more stable Thorium-mineral distribution (HEINZ, 1991). The heat source causing the mineralization (e.g. Hirschenschlag, Nebelstein) in the SBM has been obviously due to the fluid convection connected with the intrusion of biotite-granites (SLAPANSKY et al., 1993).

Due to the increasing depth to the apex of the magnetic bodies from S towards N, the increasing influence of meteoric water in the North (Hirschenschlag) on to the fluid inclusions as well as on to the ^{18}O-data and the different greisenisation and mineralization near Hirschenschlag and Nebelstein (GÖD & KOLLER, 1987; GÖD, 1989; KOLLER et al., 1992) it is obvious that in the South deeper crustal segments are exposed on surface in comparison to the North. The estimated depth difference is approximately 0.5 to 0.7 km.

7. Conclusions

Observations of P- and S-wave signals of teleseismic events by a 3 component station in Zwettl indicate a crustal thickness of about 33 km. Deep seismic sounding measurements at St. Martin near Weitra show a rather homogeneous velocity structure down to a depth of approximately 10 km. A wide band of reflected wave groups probably reflects the M-discontinuity at a depth of at least 31 km. Regarding local aspects an important result was obtained in the Messerner Bogen area. The boundary between Moldanubian (Dobra gneiss) and Moravian (Bittescher gneiss) is separated here by the Variegated Sequence. Two different tectonic hypotheses are favoured. One model suggests a link of the Bittescher gneiss and Dobra gneiss by a trough shaped structure. This is inconsistent with our geophysical results. A concordant overthrusting of Moravian formations is the more probable interpretation. This new model, which fits best the geological, seismic and magnetotelluric data, is summarised in Text-Fig. 11.

The main sources of both the magnetic and gravity anomalies are due to upper crustal structures. Over wide areas the regional anomaly pattern coincides well with tectonic structures observed at the surface. The contact zones between granitic and metamorphic rocks are clearly marked in both field distributions. The gravity reflects the lower density of the granitic intrusions relative to high density metamorphic rocks. 2D modelling shows that these intrusions are expected to extend to a depth range of about 10 km. This agrees well with the deep reflection seismic results near Nebelstein, which indicate a reasonably transparent crust. The regional gravity high at the eastern margin of the Bohemian Massif is probably due to both the Moldanubian and Moravian metamorphic rocks and a deep seated high density crustal block corresponding to the Brunovistulicum. This concept fits to the regional scale of this anomaly which extends far into the territory of the Czech Republic. In the area between Retz and Hollabrunn the Bouguer gravity is characterised by a negative-positive anomaly couple striking in a NNE–SSW direction. 2D- and 3D-modelling results explain this anomaly pattern as the combined gravity effect of the Thaya pluton and the Molasse basement, both forming a vaulted structure of the high density metamorphic crust.

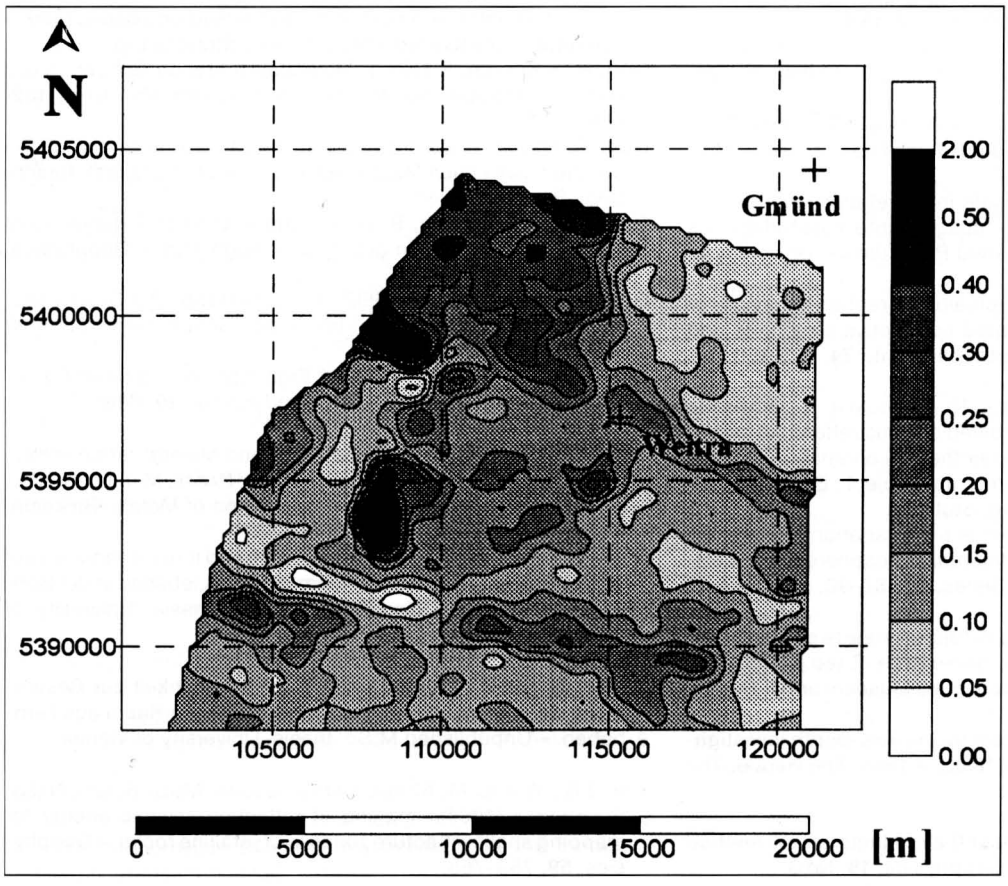

Text-Fig. 17.
The U/Th-ratio distribution [%] in the Nebelstein area (HEINZ, 1991).

The aeromagnetic map shows quiet signatures within the granitic intrusion while sequences of partly high amplitude anomalies are observed within the metamorphic part of the Moldanubian and Moravian units. The zone of magnetic anomalies in the E and SE of the SBM, already covered by young sediments, has been called the "Dunkelstein Moldanubian Belt" due to its rather striking pattern. The group of magnetic anomalies near Liebenau previously observed during the regional aeromagnetic survey was investigated in detail by a helicopter survey. The sources of these anomalies are steeply dipping contact zones between different granite types. These zones are also indicated by enrichments in potassium and partly in thorium. Under special circumstances higher uranium contents can also be observed.

Acknowledgements

Financial support of this work by the Austrian Science Foundation (FWF) projects S4701, S4710 and S4711 is gratefully acknowledged. All these projects were part of the FWF project S47–GEO "Pre-Alpine Crust in Austria". The authors wish also to thank all colleagues cooperating within the scope of S47–GEO for helpful discussions and comments.

References

ÁDÁM, A. (1987): Tectonic effects in magnetotelluric field and their numerical modelling. – Gerl. Beitr. Geophys., **96**, 17–31.

ÁDÁM, A., DUMA, G. & HORVÁTH, J. (1990): A new approach to the electrical conductivity anomalies in the Drauzug-Bakony geological unit. – Phys. Earth Planet. Int., **60**, 155–162.

ARIC, K., GUTDEUTSCH, R., LEICHTER, B., LENHARDT, W., PLOMEROVA, J., BABUSKA, V., PAJDOUSAK, P. & NIXDORF, U. (1989): Structure of the lithosphere in the Eastern Alps derived from p-residual analysis. – Arb. Zentralanstalt Met. und Geodynamik, **137**, Wien.

ARIC, K., ADAM, A. & SMYTHE, D.K. (1997): Combined seismic and magnetotelluric imaging of upper crystalline crust in the Southern Bohemian Massif. – First Break, Vol. **15**/8.

ARIC, K., FREUDENTHALER, A. & LENHARDT, W. (1992): Seismological observations in the eastern Alps. – Phys. Earth Planet. Int., **75**, 145–152.

ARIC, K., CHWATAL, W., GUTDEUTSCH, R. & JERAM, G. (1993): Seismische Struktur der Kruste in der Böhmischen Masse. – Mitt. Österr. Min. Ges., **138**, 109–117.

ARNDT, R. (1993): Drei-Dimensionale Interpretation und Visualisierung von Potentialfeldern – ausgesuchte Fallstudien aus dem Ostalpenraum. – Unpublished Ph.d. thesis, University of Vienna.

ARORA, B.R. & ÁDÁM, A. (1992): Anomalous direction behaviour or induction arrows above elongated conductive structures and its possible causes. – Phys.Earth Planet Int., **74**, 183–190.

BARTELSEN, H., LUESCHEN, E., KREY, Th., MEISSNER, R., SCHMOLL, J. & WALTER, Ch. (1982): A combined seismic reflection-refraction investigation of the Urach geothermal anomaly. – In: HAENEL, R. (ed.): The Urach Geothermal Project. E. Schweizerbart'sche Verlagsbuchhandlung, Stuttgart.

BITTNER, R. & WEVER, Th. (1991): Reflectivity variations of variscan terranes in Germany. – In: Continental Lithosphere, Deep seismic reflections. Geodynamic Series, **22**, 87–90, Am. Geoph. Union, Washington, D.C.

BRIX, F., KRÖLL, A. & WESSELY, G. (1979): Reliefkarte der Molassebasis in Niederösterreich. – In: BACHMAYER, F. (ed.): Erdöl und Erdgas in Österreich, Naturhistorisches Museum und F. Berger, Horn, Neue Folge **19**, Wien.

BRÜCKL, E. (1988): A seismic system for shallow-depth investigations. – 50th EAEG meeting, 6–10 June 1988, The Hague, The Netherlands.

CAGNIARD, L. (1953): Basic theory of the magnetotelluric method of geophysical prospecting. – Geophysics, **18**, No 3.

CHWATAL, W. (1993): Der Einfluß der Wechselwellen in der Kruste auf die Aufzeichnungen von Fernbeben. – Unpublished M.Sc. thesis, University of Vienna.

DANEU, V. (1993): Interpretation des Schwerefeldes der Kremser Bucht. – Unpublished M.Sc. thesis, University of Vienna.

DEKORP RESEARCH GROUP (1985): First Results and preliminary interpretations of deep reflection seismic recordings along profile DEKORP 2-South. – J. Geophys., **57**, 137–163.

DEKORP RESEARCH GROUP (1988): Results of the DEKORP 4/KTB Oberpfalz deep seismic reflection investigations. – J. Geophys., **62**, 69–101.

DUMA, G. & JILG, W. (1991): Gesteinsdichte und magnetische Suszeptibilität im Österreichischen Anteil der Böhmischen Masse. – Unpublished report, FWF-Projekt P7186–GEO, Inst. Met. u. Geoph., Univ. Wien.

ELEKTRB-GRUPPE c/o RAUEN, A. (1994): Untersuchungen zur elektrischen Leitfähigkeit in der Kontinentalen Tiefbohrung und ihrem Umfeld – was bringen sie uns Neues? – DGG Mittlg. **4**, 2–40.

FRITZ, H. (1991): Strukturelle Entwicklung am Südrand der Böhmischen Masse. – Proc. "Arbeitstagung der Geologischen Bundesanstalt 1991", Vienna, 89–97.

FRITZ, H. & NEUBAUER, F. (1993): Kinematics of crustal stacking and dispersion in the south-eastern Bohemian Massif. – Geol. Rdsch., **82**.

FUCHS, G. (1976): Zur Entwicklung der Böhmischen Masse. – Jb. Geol. B.-A., **119**, Wien.

FUCHS, G. & MATURA, A. (1976): Zur Geologie des Kristallins der südlichen Böhmischen Masse. – Jb. Geol. B.-A., **119**, Wien.

FUCHS, G. & MATURA, A. (1980): Die Böhmische Masse in Österreich. – In: Der Geologische Aufbau Österreichs, 121–143, Springer, Wien.

FUCHS, K. (1968): Das Reflexions- und Transmissionsvermögen eines geschichtlichen Mediums mit beliebiger Tiefen-Verteilung der elastischen Moduln und der Dichte für schrägen Einfall ebener Wellen. – Z. Geophysik, **34**, 389–413.

GIESE, P. & PRODEHL, C. (1986): Main features of the crustal structure in the central segment of the IGT based on seismic refraction data. – 3rd IGT-Workshop, 83–92, Strassbourg.

GÖD, R. & KOLLER, F. (1987): Molybdän-führende Greisen in der südlichen Böhmischen Masse. – Mitt. österr. Min. Ges., **132**, Wien.

GÖD, R. (1989): A Contribution to the Mineral Potential of the Southern Bohemian Massif (Austria). – Arch. f. Lagerst. forsch. Geol. B.-A., **11**, Wien.

GÖTZE, H. & LAHMEYER, B. (1988): Application of 3 dimensional interactive modeling in gravity and magnetics. – Geophysics, **53**, 1096–1108.

GOLTZ, G. & SCHMIDT, S. (1992): Documentation 2D-Gravity Modeling Program TALWANI. – Inst. Geol. Geoph. Geoinformatik, Freie Universität Berlin.

GUTDEUTSCH, R. & ARIC, K. (1976): Erdbeben im ostalpinen Raum. – Arb. Zentralanstalt Met. und Geodynamik, **19**, Wien.

HEINZ, H. (1991): Airborne Geophysics and Mineralization in Hercynian Granites of Central Europe. – In: PAGEL, M. & LEROY, J.L. (eds.): Source, Transport and Deposition of Metals, Balkema, Rotterdam.

HÜBL, G. (1993): Modellrechenmethoden und ihre Anwendung auf eine Gruppe magnetischer Anomalien bei Liebenau in der Böhmischen Masse. – Unpublished M.Sc. thesis, University of Vienna.

JERAM, G. (1992): Eine Diskussion der Möglichkeit zur Bestimmung der Lithosphärenstruktur im ostalpinen Raum aus Fernbeben. – Unpublished M.Sc. thesis, University of Vienna.

KIM, J.S., WOOIL, M. MOON, GANPAL LODHA, MULU SERZU, NASH, SOONAWALA (1994): Imaging of reflection seismic energy for mapping shallow fracture zones in crystalline rocks. – Geophysics, **59**, 753–765.

KLOB, H. (1970): Über das Vorkommen eines porphyrischen Granites im Raume Sandl – Karlstift – Liebenau bei Freistadt im oberösterreichischen Mühlviertel (Granit vom Typ Karlstift). – TMPM, **14**, Wien.

KOLLER, F., HÖGELSBERGER, H. & KOEBERL, C. (1992): Fluid-rock interaction in the Mo-bearing greisen complex Nebelstein, Bohemian Massif (Austria). – Mineralogy Petrology, **45**, Springer, Wien.

KRAIGER, G. (1988): Influence of the curvature parameter on least-squares prediction. – Manuscripta geodaetica, **13**, 164–171.

LIBOWITZKY, E. (1989): Mineralogische Untersuchungen einer magnetischen Anomalie im Moravikum der Böhmischen Masse in Österreich. – Unpubl. thesis, University of Vienna.

MEISSNER, R. & DEKORP RESEARCH GROUP (1991): The Dekorp Surveys: Major Results in tectonic and reflective styles. – In: Continental Lithosphere; Deep seismic reflections, Geodynamic Series, **22**, 69–76, Am. Geoph. Union, Washington, D.C.

MEISSNER, R., BARTELSEN, H., KREY, T. & SCHOLL, J. (1982): Detecting velocity anomalies in the region of the Urach geothermal anomaly by means of new seismic field arrangements. – In: CERMAK, V. & HAENEL, R. (eds): Geothermics and geothermal energy, 285–292, E. Schweizerbart'sche Verlagsbuchhandlung, Stuttgart.

MEISSNER, R., SPRINGER, M. & FLUCH, E. (1984): Tectonics of the Variscides in North-Western Germany based on seismic reflection measurements. – In: HUTTON, D.H.W. & SANDERSON, D.J. (eds.): Variscan Tectonics of the North Atlantic region. Blackwell, London.

MEURERS, B. (1990): Gravity investigations in the Austrian part of the Bohemian massif. – Proc. "Advances in Gravimetry", Smolenice (CSFR), 51–56.

MEURERS, B. (1991): First attempt of gravity map stripping in the south-eastern part of the Bohemian Massif. – Proc. Arbeitstagung der Geologischen Bundesanstalt 1991, Vienna.

MEURERS, B. (1993): Die Böhmische Masse Österreichs im Schwerebild. – 6. Int. Alpengrav. Koll., Leoben 1993, Beitr. Österr. Met. Geoph., **7**, 69–81.

MEURERS, B. & STEINHAUSER, P. (1990): Die Bouguer-Anomalie am Ostrand der Böhmischen Masse. – Beitr. Österr. Met. Geoph., **3**, 13–23.

MEURERS, B. & STROBL, Ch. (1993): Analyse des Schwerefeldes der südlichen Böhmischen Masse durch gravimetrisches Stripping und Dichte-Dekonvolution. – Mitt. Österr. Min. Ges., **138**, 227–235.

MEURERS, B., STEINHAUSER, P., WALACH, G. & FRITZER, J. (1991): A new gravity map in the southern part of the Bohemian Massif. – XXth General Assembly IUGG, Wien 1991.

MEURERS, B., ARIC, K., BRÜCKL, E. & STEINHAUSER, P. (1993): Seismische Untersuchung der Untergrundstruktur der Molasse am Ostrand der Böhmischen Masse. – Unpubl. report, **32**, Institute Meteorology and Geophysics, University of Vienna.

MORITZ, H. (1980): Geodetic reference system 1980. – Bull. Geod., **54**, 3, 395–405.

MOTSCHKA, K. (1995): Anwendung der Faktorenanalyse auf die Aero-Radiometrie im Raum Weitra, Nebelstein und Freistadt. – Unpubl. M.Sc. thesis, University of Vienna.

PALMER, D. (1981): An introduction to the generalized reciprocal method of seismic refraction interpretation. – Geophysics, **46**, No. 11.

PARKER, R.L. (1972): The rapid calculation of potential anomalies. – Geophys. J. R. Astr. Soc., **31**, 447–455.

PARKINSON, W.D. (1962): The influence of continents and oceans on the geomagnetic variations. – Geophys. J. R. Astr. Soc., **6**, 441–449.

POSGAY, K., ALBU, I., MAYEROVA, M., NAKLADALOVA, Z., IBRMAJER, I., BLIZKOVSKY, M., ARIC, K. & GUTDEUTSCH, R. (1991): Contour Map of the Mohorovicic Discontinuity beneath Central Europe. – Geoph. Transactions, **36**, 7–13.

PRICHYSTAL, A. (1993): Geologische Aufnahmen im SBP. – In: HEINZ, H. (ed.): Verifizierung und fachliche Bewertung von Forschungsergebnissen und Anomaliehinweisen aus regionalen und überregionalen Basisaufnahmen und Detailprojekten, Bericht ÜLG-28/92, GBA-Archiv Nr. 10073, Wien.

PRICHYSTAL, A. & LOSOS, Z. (1993): Analyse der opaken Mineralphasen aus Anschliffen von ausgewählten Proben aus dem Südböhmischen Pluton. – In: HEINZ, H. (ed.): Verifizierung und fachliche Bewertung von Forschungsergebnissen und Anomaliehinweisen aus regionalen und überregionalen Basisaufnahmen und Detailprojekten, Bericht ÜLG-28/92, GBA-Archiv Nr. 10073, Wien.

RADINGER, A. (1994): Modellrechnungen am Ostrand der Böhmischen Masse. – Unpubl. Dissertation, Universität Wien.

ROETZEL, R. (1989): Bohrungen im Bereich von Krems und Herzogenburg. – Geol. B.-A., Wien.

RUESS, D. (1988): Stand des Österreichischen Schweregrundnetzes und des digitalen Geländemodells. – 4. Int. Alpengrav. Koll., Wien 1986, Ber. Tiefbau Ostalpen, **13**, Zentralanstalt Met. u. Geodynamik, Wien, 323, 159–164.

SCHRAUDER, M., BERAN, A., FÖRNESS, S. & RICHTER, W. (1993): Constraints on the origin and the genesis of graphite bearing rocks of the variegated sequence of the Bohemian Massif. – Mineralogy and Petrology, **49**, 175–188

SEIBERL, W. & HEINZ, H. (1990): Interpretationsmethoden in der Magnetik anhand von Beispielen aus der Böhmischen Masse. – Österr. Beitr. Met. Geophys., **3**, 43–56.

SENFTL, E. (1965): Schwerekarte von Österreich, 1 : 1.000.000. – BEV, Wien.

SLAPANSKY, P., HÖGELSBERGER, H., KOLLER, F., HEINZ, H., GÖD, R. & FALLICK, A.E. (1993): Hydrothermal Alterations of Granites in the South Bohemian Pluton. – Fluid-Info, Leoben.

SMYTHE, D.K. (1994): Preliminary processing of high resolution data from the Bohemian Massif, Austria. – Unpubl. report, Dept. Geology and Applied Geology, Univ. of Glasgow, 24 pp.

STEINER, T. (1989): MT inversion using least-absolute-values and least squares. – Abstracts and Papers of the Technical Program, 34. Geofizikai Szimpuzium, Budapest. 1989 sept. 4–8, 639–651.

STEINHAUSER, P., RUESS, D., ZYCH, D., HAITZMANN, H. & WALACH, G. (1984a): The Geoid in Austria. Digital models of mean topographic heights and rock densities. – Proc. XVIIIth General Assembly of the IUGG, IAG, Vol. 1, 322–338.

STEINHAUSER, P., MEURERS, B. & ARIC, K., GRANSER, H., LENHARDT, W. & KLINGER, G. (1984b): Geophysikalische Erkundung der Untergrundstrukturen der Kremser Bucht. – Unpubl. report, **14**, Institute Meteorology and Geophysics, University of Vienna.

STEINHAUSER, P., MEURERS, B., BRÜCKL, E. & ARIC, K. (1985): Geophysikalische Erkundung der Untergrundstrukturen der Herzogenburger Bucht. – Unpubl. report, **16**, Institute Meteorology and Geophysics, University of Vienna.

STEINHAUSER, P., BRÜCKL, E., MEURERS, B. (1986): Geophysikalische Untersuchung des Molasseschelfs im Raum Retz. – Unpubl. report, **21**, Institute Meteorology and Geophysics, University of Vienna.

STEINHAUSER, P., MEURERS, B. & BRÜCKL, E. (1987): Geophysikalische Untersuchung des Molasseschelfs im Raum Röschitz. – Unpubl. report, **23**, Institute Meteorology and Geophysics, University of Vienna.

STROBL, Ch. (1993): Untersuchung der Schwerewirkung des Österreichischen Anteils der Böhmischen Masse. – Unpubl. M.Sc. thesis, University of Vienna.

STRÖSSENREUTHER, U. (1982): Die Struktur der Erdkruste am Südwestrand der Böhmischen Masse abgeleitet aus refraktionsseismischen Messungen der Jahre 1970 und 1978/79. – Unpubl. Ph.d. thesis, Ludwig-Maximilian University Munich.

SÜNKEL, H. (1980): A general surface representation module designed for geodesy. – Ohio State University, Report No. **292**.

THIELE, O. (1976): Ein westvergenter kaledonischer Deckenbau im niederösterreichischen Waldviertel? – Jb. Geol. B.-A., **119**, 75–83, Wien.

TOMEK, C., DVORAKOVA, L. & IBRMAJER, I. (1987): Crustal profiles of active continental collisional belt: Czechoslovak deep seismic reflection profiling in the West Carpathians. – Geophys. J. R. Astr. Soc., **89**, 383–388.

TOMEK, C., DVORAKOVA, V., NOVOTNY, M. & VEJMELEK, L. (1993): Interpretation of seismic data from profiles 9HR/91 503M/92 and VI/70. – Internal report UUG Praha by Kappe, Brno, 63 p., in Czech.

TREITEL, S. & ROBINSON, E.A. (1966): Seismic wave propagation in layered media in terms of communication theory. – Geophysics, **31**, 17–32.

WALACH, G. (1987): A digital model of surface rock densities of Austria and the Alpine realm. – In: The gravity field in Austria. Geod. Arb. Österr. Int. Erdmessung, Neue Folge, Band IV, 3–9, Österr. Komm. Int. Erdmessung, Graz.

WALACH, G. (1990): Schwerefeldbestimmung im westlichen Mühlviertel – Erste Ergebnisse. – Beitr. Österr. Met. Geoph., **3**, 5–11.

WENZEL, H.G. (1985): Hochauflösende Kugelfunktionsmodelle für das Gravitationspotential der Erde. – Wiss. Arb. Univ. Hannover, No. 137.

WIESENEDER, H. & FREILINGER, G. (1976): Der kristalline Untergrund der Nordalpen in Österreich. – Geolog. Rdsch., **65**, Stuttgart.

Manuskript bei der Schriftleitung eingelangt am 11. April 1997

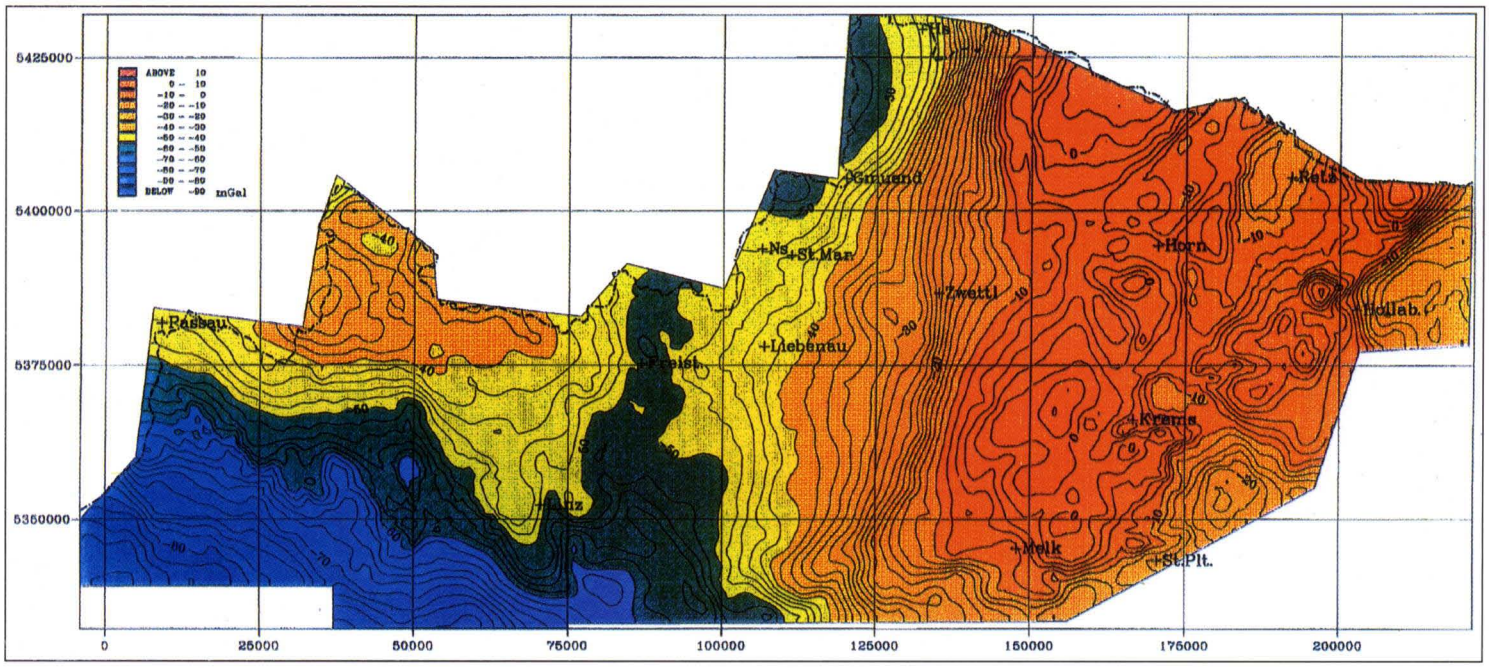

Fig. 1.
Bouguer gravity map of the Southern Bohemian Massif (MEURERS et al., 1991).

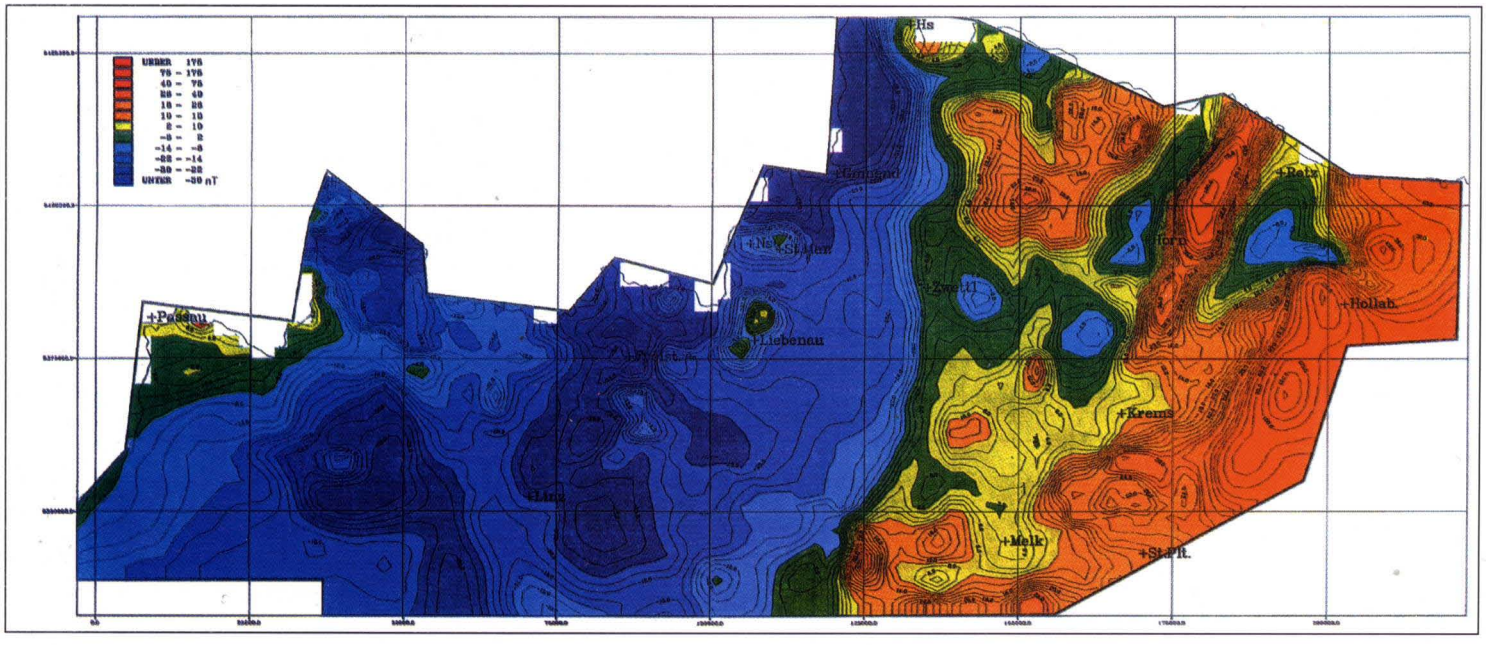

Fig. 2.
Magnetic Map.

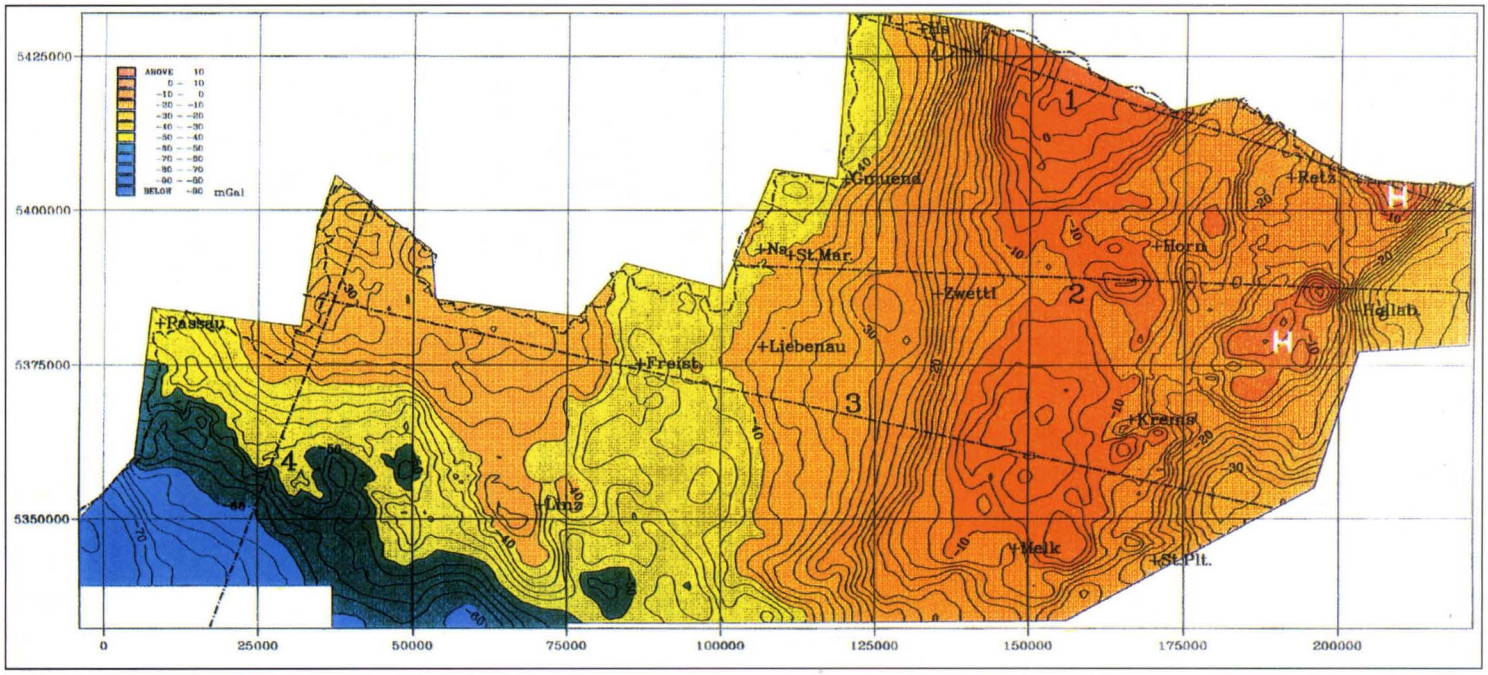

Fig. 1.
Stripped Bouguer gravity map of the Southern Bohemian Massif (MEURERS &STROBL, 1993).
Mass corrections according to a lateral density model, gravitational effect of Moho undulation subtracted.
Numbered lines indicate 2D-modelling profiles (see Text-Figs. 13, 14).

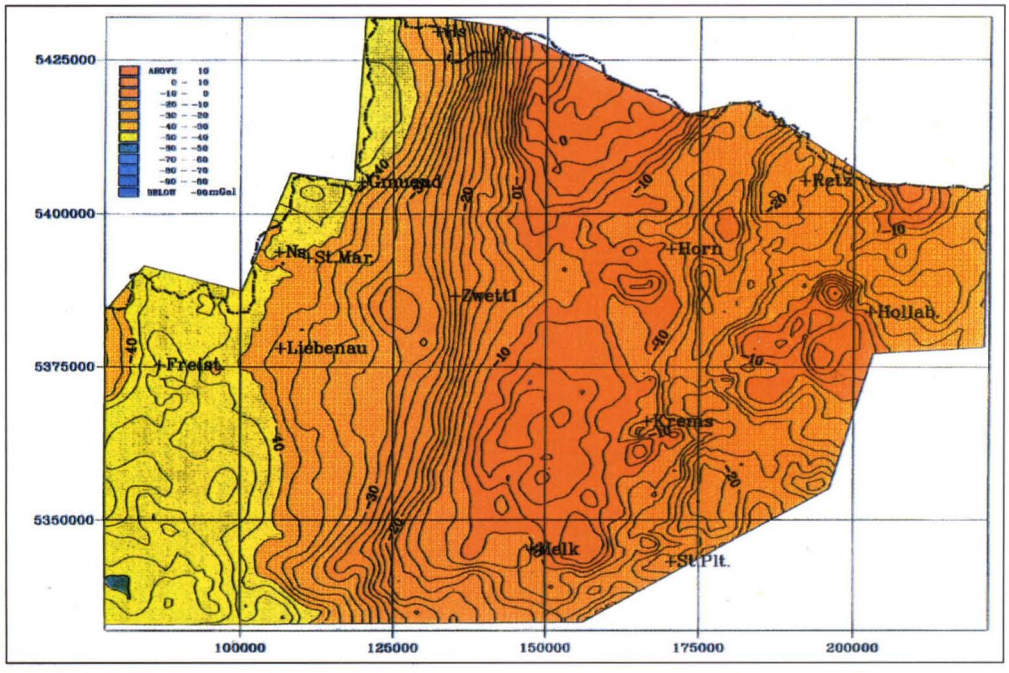

Fig. 2.
Stripped Bouguer gravity map of the Eastern margin of the Southern Bohemian Massif (MEURERS &STROBL, 1993).
Mass corrections according to a lateral density model, gravitational effect of Moho undulation and Molasse sediments subtracted.